Endothelial-to-mesenchymal transition contributes to endothelial dysfunction and dermal fibrosis in systemic sclerosis

Annals of the
RHEUMATIC DISEASES
The Eular Journal

Endothelial-to-mesenchymal transition contributes to endothelial dysfunction and dermal fibrosis in systemic sclerosis

Journal:	*Annals of the Rheumatic Diseases*
Manuscript ID	annrheumdis-2016-210229.R1
Article Type:	Extended report
Date Submitted by the Author:	15-Nov-2016
Complete List of Authors:	Manetti, Mirko; University of Florence, Experimental and Clinical Medicine, Section of Anatomy and Histology Romano, Eloisa; University of Florence, Experimental and Clinical Medicine, Section of Internal Medicine, Rheumatology Unit Rosa, Irene; University of Florence, Experimental and Clinical Medicine, Section of Anatomy and Histology Guiducci, Serena; University of Florence, Experimental and Clinical Medicine, Section of Internal Medicine, Rheumatology Unit Bellando-Randone, Silvia; University of Florence, Experimental and Clinical Medicine, Section of Internal Medicine, Rheumatology Unit de Paulis, Amato; University of Naples Federico II, Department of Translational Medical Sciences and Center for Basic and Clinical Immunology Research (CISI) Ibba-Manneschi, Lidia; University of Florence, Experimental and Clinical Medicine, Section of Anatomy and Histology Matucci-Cerinic, Marco; University of Florence, Experimental and Clinical Medicine, Section of Internal Medicine, Rheumatology Unit
Keywords:	Systemic Sclerosis, Qualitative research, Fibroblasts

Endothelial-to-mesenchymal transition contributes to endothelial dysfunction and dermal fibrosis in systemic sclerosis

Mirko Manetti,[1] Eloisa Romano,[2] Irene Rosa,[1,2] Serena Guiducci,[2] Silvia Bellando-Randone,[2] Amato De Paulis,[3] Lidia Ibba-Manneschi,[1] Marco Matucci-Cerinic[2]

[1]Department of Experimental and Clinical Medicine, Section of Anatomy and Histology, University of Florence, Florence, Italy

[2]Department of Experimental and Clinical Medicine, Section of Internal Medicine, Rheumatology Unit, Azienda Ospedaliero-Universitaria Careggi (AOUC), University of Florence, Florence, Italy

[3]Department of Translational Medical Sciences and Center for Basic and Clinical Immunology Research, University of Naples Federico II, Naples, Italy

Correspondence to

Dr Mirko Manetti,

Department of Experimental and Clinical Medicine,

Section of Anatomy and Histology,

University of Florence,

Largo Brambilla 3,

Florence 50134, Italy;

mirkomanetti@yahoo.it,

mirko.manetti@unifi.it

ABSTRACT

Objective: Systemic sclerosis (SSc) features multiorgan fibrosis orchestrated predominantly by activated myofibroblasts. Endothelial-to-mesenchymal transition (EndoMT) is a transdifferentiation by which endothelial cells (ECs) lose their specific morphology/markers and acquire myofibroblast-like features. Here, we determined the possible contribution of EndoMT to the pathogenesis of dermal fibrosis in SSc and two mouse models.

Methods: Skin sections were immunostained for endothelial CD31 or VE-cadherin in combination with α-smooth muscle actin (α-SMA) myofibroblast marker. Dermal microvascular ECs (dMVECs) were prepared from SSc and healthy skin (SSc-dMVECs and H-dMVECs). H-dMVECs were treated with transforming growth factor-β1 (TGFβ1) or SSc and healthy sera. Endothelial/mesenchymal markers were assessed by real-time PCR, immunoblotting and immunofluorescence. Cell contractile phenotype was assayed by collagen gel contraction.

Results: Cells in intermediate stages of EndoMT were identified in dermal vessels of either SSc patients or bleomycin-induced and urokinase-type plasminogen activator receptor (uPAR)-deficient mouse models. At variance with H-dMVECs, SSc-dMVECs exhibited a spindle-shaped appearance, coexpression of lower levels of CD31 and VE-cadherin with myofibroblast markers (α-SMA+ stress fibres, S100A4 and type I collagen), constitutive nuclear localisation of the EndoMT driver Snail1 and an ability to effectively contract collagen gels. Treatment of H-dMVECs either with SSc sera or TGFβ1 resulted in the acquisition of a myofibroblast-like morphology and contractile phenotype and downregulation of endothelial markers in parallel with the induction of mesenchymal markers. Matrix metalloproteinase-12-dependent uPAR cleavage was implicated in the induction of EndoMT by SSc sera.

Conclusions: In SSc, EndoMT may be a crucial event linking endothelial dysfunction and development of dermal fibrosis.

Keywords: systemic sclerosis, dermal microvascular endothelial cells, myofibroblasts, endothelial-to-mesenchymal transition, dermal fibrosis

INTRODUCTION

Systemic sclerosis (SSc) is a complex connective tissue disease of unknown aetiology characterised by widespread peripheral microvascular injury evolving into progressive fibrosis of skin and multiple internal organs [1-3]. In SSc, fibrosis results from an unrestrained tissue repair process orchestrated predominantly by activated myofibroblasts that are a population of mesenchymal cells displaying unique biological functions. These include an increased synthesis of fibrillar type I and III collagens, a reduction in the expression of genes encoding extracellular matrix (ECM)-degrading enzymes and α-smooth muscle actin (α-SMA) expression and incorporation into stress fibres, which provides an increased contractile force that is crucial for their tissue remodelling properties [4-6]. Indeed, myofibroblast contraction contributes to a large extent to a progressive increase in connective tissue stiffness, a recently recognised potent profibrotic stimulus [7-10].

Given the crucial role of myofibroblasts in the pathogenesis of organ fibrosis in a variety of disorders, considerable attention has been paid to the identification of their putative cellular origins. Hence, extensive investigations have revealed that profibrotic myofibroblasts may arise from different sources including expansion and activation of resident tissue fibroblasts and perivascular pericytes, recruitment of bone marrow-derived circulating precursors, transformation of white adipocytes and transdifferentiation of epithelial cells into mesenchymal cells [4,11-13]. More recently, it has been reported with increasing frequency that vascular endothelial cells (ECs) may also exhibit substantial plasticity by undergoing endothelial-to-mesenchymal transition (EndoMT), a transdifferentiation by which ECs disaggregate, lose polarity and acquire ECM-producing myofibroblast features [14-16]. EndoMT is a phenotypical conversion in which ECs downregulate the expression of their specific markers, such as CD31/platelet-EC adhesion molecule-1, von Willebrand factor (vWF) and vascular endothelial (VE)-cadherin, and acquire mesenchymal cell products including α-SMA, S100A4/fibroblast-specific protein-1 (FSP1) and type I collagen, together with stabilisation and nuclear translocation of the transcriptional regulator Snail1, a crucial trigger of mesenchymal transition [14-16].

To date, EndoMT has emerged as a player in the pathogenesis of tissue fibrosis and fibroproliferative vasculopathy in various diseases, including diabetic nephropathy, cardiac fibrosis, inflammatory bowel disease-related intestinal fibrosis, portal hypertension and primary pulmonary arterial hypertension (PAH) [14,16-21]. Of note, extensive research studies have shown that multiple pathways implicated in SSc pathogenesis, such as transforming growth factor-β (TGFβ), endothelin-1 (ET-1), Notch, Sonic Hedgehog and Wnt pathways, as well as other putative pathways such as oxidative stress and hypoxia, may participate in the molecular mechanisms of the EndoMT

process [16]. For instance, EndoMT can be fully induced by TGFβ in cultured ECs from different tissues [20,22-24].

Although recent studies support the notion that EndoMT may participate in the development of SSc-associated interstitial lung disease (ILD) and PAH [25,26], the occurrence of such a phenotypical change from ECs to activated myofibroblasts has never been demonstrated in the affected skin of SSc patients. Therefore, in the present study we combined ex vivo, in vitro and in vivo approaches to investigate the possible contribution of EndoMT to the pathogenesis of dermal fibrosis in SSc and two mouse models of the disease.

MATERIALS AND METHODS

An extended methods section is provided in the online supplementary material.

Cell culture and reagents

Primary cultures of dermal microvascular ECs (dMVECs) were established by explantation from biopsies of the lesional forearm skin from 6 patients with early diffuse cutaneous SSc (dcSSc; disease duration <2 years from first non-Raynaud symptom) [27] and from 6 healthy adult subjects under protocols approved by the local institutional review board at the Azienda Ospedaliero-Universitaria Careggi (AOUC), Florence, Italy. Skin biopsies were processed as previously described [28,29]. Patient characteristics are summarised in online supplementary table S1. Adherent cells were detached and subjected to CD31 immunomagnetic isolation by incubation with anti-CD31 conjugated-microbeads [28,29]. Isolated cells were further identified as ECs by labelling with anti-factor VIII-related antigen (vWF) and anti-CD105, followed by reprobing with anti-CD31 antibodies (see online supplementary figure S1). dMVECs from healthy subjects (H-dMVECs) and SSc patients (SSc-dMVECs) were maintained as detailed in the online supplementary material. In selected experiments, H-dMVECs were treated with recombinant human TGFβ1 (10 ng/ml; PeproTech, Rocky Hill, NJ, USA) or 10% serum from early dcSSc patients (n=6) and healthy subjects (n=6) for 24, 48 and 72 hours. In some experimental points, sera were preincubated with the matrix metalloproteinase-12 (MMP-12) specific inhibitor MMP408 (10 nM; Sigma-Aldrich, St. Louis, MO, USA) before cell stimulation.

Fluorescence immunocytochemistry

At the end of the experiments, cells were fixed with 3.7% buffered paraformaldehyde and immunofluorescence with antibodies against CD31, VE-cadherin, α-SMA, S100A4/FSP1, type I

collagen and Snail1 (all from Abcam, Cambridge, UK) was performed as detailed in the online supplementary material. In some specimens, Alexa 488-labelled phalloidin (Invitrogen, Carlsbad, CA, USA) was applied to the cells to visualise the arrangement of the F-actin cytoskeleton. For primary and secondary antibodies, refer to the online supplementary material.

RNA isolation and quantitative real-time PCR

At the end of the experiments, cultures were harvested and total RNA was isolated using the RNeasy Micro Kit (Qiagen, Milan, Italy). First strand cDNA synthesis and mRNA quantification by SYBR Green real-time PCR were performed as reported elsewhere [29]. For predesigned oligonucleotide primer pairs, refer to the online supplementary material.

Immunoblotting

Whole cell protein lysates from dMVECs were subjected to immunoblot analysis as described elsewhere [29]. For details on primary antibodies against CD31, VE-cadherin, α-SMA, S100A4/FSP1, type I collagen, Snail1, Friend leukemia integration-1 (Fli1), urokinase-type plasminogen activator receptor (uPAR) domain 1 (D1) and domain 2 and α-tubulin, refer to the online supplementary material.

Collagen gel contraction assay

Collagen gel contraction assays were performed as described in the online supplementary material.

Enzyme-linked immunosorbent assay

Levels of MMP-12 in serum samples were measured by quantitative enzyme-linked immunosorbent assay as described in the online supplementary material.

Fluorescence immunohistochemistry on human and mouse skin

Paraffin-embedded sections of lesional forearm skin biopsies were obtained from 12 SSc patients (n=4 with limited cutaneous SSc and n=8 with dcSSc) and 10 age-matched and gender-matched healthy donors, as described elsewhere [28-30]. Skin sections from two mouse models of dermal fibrosis were also used. First, 6 week-old male C57BL/6 mice (Charles River Laboratories, Calco, Lecco, Italy) received subcutaneous injections of 100 µl of bleomycin dissolved in 0.9% NaCl (saline solution) at a concentration of 0.5 mg/ml every other day for 4 weeks in well-defined areas of the upper back. Subcutaneous injections of 0.9% NaCl served as controls [31]. The second model consisted of 12 week-old male uPAR-deficient mice and wild-type littermates as described

elsewhere [32,33]. All animal protocols were performed in accordance with DL 116/92 and approved by the Institutional Animal Care and Use Committee of the University of Florence. Each experimental group consisted of at least six mice. Double-label immunofluorescence using antibodies against α-SMA and CD31 or VE-cadherin was carried out as detailed in the online supplementary material. The percentage of dermal vessels displaying CD31/α-SMA and VE-cadherin/α-SMA colocalisation was determined in five randomly selected high-power fields of the dermis from each of three sections per sample.

Transmission electron microscopy

Ultrathin skin sections from 5 dcSSc patients and 5 healthy controls were processed and examined according to previously published protocols [34] as detailed in the online supplementary material.

Statistical analysis

Statistical analyses were performed using the Statistical Package for Social Sciences software for Windows, V.20.0 (SPSS, Chicago, IL, USA). Data are expressed as means and standard errors of the mean (SEM). The Student's t-test was used for statistical evaluation of the differences between two independent groups. A p value of <0.05 according to a two-tailed distribution was considered statistically significant.

RESULTS

EndoMT in dermal vessels of SSc patients and experimental models of SSc

In order to determine ex vivo the presence of transitional EndoMT cells, skin sections from SSc patients and healthy donors were subjected to double immunofluorescence staining for the EC markers CD31 or VE-cadherin and the myofibroblast marker α-SMA. In the healthy dermal microvasculature, α-SMA expression was mostly restricted to pericytes and vascular smooth muscle cells surrounding the endothelial layer (figure 1A). On the contrary, we observed colocalised CD31/α-SMA and VE-cadherin/α-SMA in the endothelium of numerous dermal capillary vessels and arterioles from SSc patients, suggestive for cells in intermediate stages of EndoMT (figure 1A). Indeed, the percentage of vessels displaying CD31/α-SMA and VE-cadherin/α-SMA colocalisation was significantly increased in skin biopsies from SSc patients compared with healthy skin ($p<0.001$ for both) (figure 1B). No difference in the frequency of transitional EndoMT cells was observed between SSc cutaneous subsets (data not shown). Furthermore, transmission electron microscopy

analysis revealed that the presence of vWF-storing Weibel-Palade bodies was clearly reduced in SSc dermal endothelium (figure 1C).

Next we investigated in vivo the presence of transitional EndoMT cells in the skin of two mouse models of SSc, namely mice with bleomycin-induced dermal fibrosis and uPAR-deficient mice [31-33]. The frequency of transitional EndoMT cells in murine skin was assessed by colocalisation of either CD31 or VE-cadherin and α-SMA. As displayed in figure 2, using both marker combinations we observed transitional EndoMT cells to be present at very low levels in saline-treated control mice, with significantly higher levels in the bleomycin treatment group ($p<0.001$ for both). Similarly, a significantly higher percentage of vessels with CD31/α-SMA and VE-cadherin/α-SMA double-positive cells was detected in the dermis of uPAR-deficient mice compared with wild-type littermates ($p<0.001$ for both) (figure 2A,B).

Cultured SSc-dMVECs coexpress endothelial and mesenchymal cell markers and exhibit a myofibroblast-like functional phenotype

The expression of endothelial and mesenchymal cell markers in dMVECs isolated from forearm skin biopsies was investigated by immunofluorescence and immunoblotting. In agreement with previous reports [28,35], H-dMVECs exhibited a typical endothelial morphology with a polygonal shape, whereas the majority of SSc-dMVECs had an elongated shape often characterised by branches (figure 3A). Both H-dMVECs and SSc-dMVECs were immunopositive for the pan-EC marker CD31 (figure 3A). However, the expression of CD31 and VE-cadherin was markedly decreased in SSc-dMVECs compared with H-dMVECs (figure 3A). SSc-dMVECs also expressed α-SMA, which often was incorporated into stress fibres, as well as S100A4/FSP1 and type I collagen (figure 3A). On the contrary, as expected, in H-dMVECs there was no evidence of α-SMA and type I collagen expression, and S100A4/FSP1 was almost undetectable (figure 3A). Double immunofluorescence staining clearly revealed the unique presence of numerous CD31+ cells displaying α-SMA+ stress fibres in SSc-dMVEC cultures compared with H-dMVECs ($p<0.001$) (figure 3B). Phalloidin staining further revealed that while H-dMVECs showed a weak and disorganised expression of F-actin fibres, SSc-dMVECs exhibited a marked increase in stress fibres mainly organised longitudinally (figure 3A). Furthermore, we investigated the expression of Snail1, a zinc-finger transcription factor that induces numerous transcriptional events leading to the acquisition of a mesenchymal cell-specific phenotype such as stimulation of α-SMA expression [16,24]. As displayed in figure 3A, strong expression and nuclear localisation of Snail1 were constitutively detected in SSc-dMVECs, while Snail1 expression was negligible in H-dMVECs. Immunoblot analyses confirmed either a significantly lower protein expression of CD31 and VE-

cadherin or a significantly higher expression of α-SMA, S100A4/FSP1, type I collagen and Snail1 in SSc-dMVECs compared with H-dMVECs ($p<0.001$ for all comparisons) (figure 3C). According to the immunofluorescence data, both α-SMA and type I collagen were undetectable in protein lysates from H-dMVECs (figure 3C). Moreover, SSc-dMVECs exhibited a significant reduction in protein expression of Fli1 ($p<0.001$ versus H-dMVECs) (figure 3C), a transcription factor which plays a pivotal role in the maintenance of EC homeostasis and whose deficiency may be implicated in EndoMT [36-38]. The occurrence of EndoMT was confirmed functionally by the evidence that SSc-dMVECs were able to effectively contract collagen gels (figure 3D).

Treatment with SSc sera induces a myofibroblast-like phenotype in H-dMVECs

Previous studies have demonstrated that treatment with sera from SSc patients impairs the angiogenic performance of H-dMVECs in vitro [29,39,40]. Nevertheless, whether these antiangiogenic effects may be in part related to the induction of the EndoMT process has never been investigated. To address this issue, H-dMVECs were challenged with sera from early dcSSc patients and healthy subjects and subsequently assayed for changes in cell morphology and the expression of endothelial and mesenchymal cell markers. According to the literature [20,22-24], stimulation with recombinant human TGFβ1 was performed in parallel as a positive control of EndoMT. After 48-hour treatment with SSc sera, H-dMVECs started to disaggregate losing their characteristic polygonal cobblestone-like morphology (figure 4A). These changes progressed rapidly with the appearance of numerous cells exhibiting a spindle-shaped morphology in H-dMVEC cultures treated with SSc sera for 72 hours (figure 4A). As expected, similar findings were observed when H-dMVECs were challenged with TGFβ1, whereas H-dMVEC morphology did not change over time in cultures treated with healthy sera (figure 4A). Indeed, 72-hour treatment either with SSc sera or TGFβ1 induced a significant increase in the percentage of spindle-shaped cells (both $p<0.001$ versus basal H-dMVECs) (figure 4A) which were able to effectively contract collagen gels (figure 4B).

As displayed in figure 5, real-time PCR analysis revealed a significant reduction in mRNA levels of *CD31*, *CDH5* and *FLI1* genes in H-dMVECs treated either with SSc sera or TGFβ1 for 48 hours (all $p<0.001$ versus basal H-dMVECs). This happened in parallel with the induction of *ACTA2*, *S100A4*, *SNAI1*, *COL1A1* and *COL1A2* mRNA expression (all $p<0.001$ versus basal H-dMVECs) (figure 5). On the contrary, 48-hour treatment of H-dMVECs with healthy sera did not affect mRNA expression levels of the aforementioned markers (figure 5). These results were confirmed by immunoblot and immunofluorescence assessment of endothelial and mesenchymal protein expression levels in cells treated for 72 hours (figure 6A-G). In particular, both untreated cells and

those treated with healthy sera showed no expression of α-SMA and type I collagen along with very low levels of Snail1, whereas treatment either with SSc sera or TGFβ1 induced the appearance of α-SMA+ stress fibres, de novo synthesis of type I collagen and strong expression and nuclear localisation of Snail1 (figure 6B-G).

MMP-12-dependent cleavage of uPAR is implicated in the induction of EndoMT by SSc sera

We previously demonstrated that in SSc-dMVECs, uPAR undergoes a MMP-12-dependent cleavage of domain D1 resulting in impaired angiogenesis [35,41]. Interestingly, the cleavage of uPAR-D1 was shown to be a crucial step in fibroblast-to-myofibroblast transition [42]. Therefore, we herein investigated whether MMP-12-dependent uPAR-D1 cleavage could be implicated in the induction of EndoMT by SSc sera. Consistent with previous reports [40,43], MMP-12 levels were raised in SSc sera (see online supplementary figure S2A). Treatment of H-dMVECs with SSc sera resulted in uPAR-D1 cleavage already after 24 hours (see online supplementary figure S2B). Such a cleavage was instead prevented when SSc sera were preincubated with the MMP-12 specific inhibitor MMP408 (see online supplementary figure S2B). As shown in online supplementary figure S3, preincubation with MMP408 significantly blunted the effects of 48-hour treatment with SSc sera on gene expression of endothelial and mesenchymal cell markers.

DISCUSSION

Our data provide the first direct evidence that EndoMT may take place in the skin of SSc patients and may have therefore a role in the pathogenesis of dermal fibrosis. The ex vivo immunohistological data clearly demonstrate the presence of transitional EndoMT cells simultaneously expressing EC and myofibroblast markers in SSc dermal microvasculature. In contrast, EndoMT was only observed at negligible levels in control skin. These results are substantially in agreement with similar findings recently described in the pulmonary vessels of patients with SSc-associated ILD and PAH [25,26]. We have further characterised in vitro the phenotype of dMVECs isolated from SSc skin and found that these cells are in an intermediate state between an EC and a myofibroblast-like contractile phenotype, combining markers of both cell types. The results also show that H-dMVECs can undergo EndoMT in response to treatment with SSc sera, thus supporting the hypothesis that such cellular transdifferentiation may be operative in SSc. In fact, after a prolonged challenge with SSc sera, H-dMVECs lost their typical endothelial cobblestone appearance and acquired myofibroblast-like structural and functional features. Consistent with these morphofunctional changes, SSc serum-treated H-dMVECs exhibited a reduction in the expression of EC markers CD31 and VE-cadherin and an upregulation of

mesenchymal markers, including α-SMA+ stress fibres, S100A4/FSP1, type I collagen and nuclear Snail1. Furthermore, the presence of transitional EndoMT cells in dermal vessels of two murine models of SSc is a matter of interest. Indeed, previous studies have demonstrated the occurrence of EndoMT in animal models of cardiac, pulmonary and renal fibrosis, as well as in models of PAH [16,23,26,44,45]. Although our experimental data support the notion that EndoMT may contribute to the accumulation of myofibroblasts and the development of dermal fibrosis in vivo, this needs to be further confirmed by using lineage tracing in different preclinical models of SSc.

Besides the increase in the number of profibrotic myofibroblasts, EndoMT may favour microvascular derangement and loss of ECs contributing to capillary rarefaction, impaired angiogenesis and chronic tissue ischaemia in SSc skin. Indeed, endothelial dysfunction is considered a pivotal factor contributing to peripheral vessel remodelling in SSc [3,15,41]. A defective response to proangiogenic stimuli and several functional defects, such as an impaired ability to organise into capillary-like tubes in vitro, have been extensively reported in SSc-dMVECs [28,29,35,41,46]. Moreover, transcriptome profiling studies have revealed profound differences in the expression of genes encoding a variety of angiogenic regulators between SSc-dMVECs and H-dMVECs [41,47]. In this context, our present findings shed light on EndoMT as a pathogenic mechanism that in SSc may directly link EC dysfunction to the development of dermal fibrosis. The intrinsic propensity of SSc-dMVECs to transition towards a profibrotic myofibroblast-like phenotype might in effect largely explain their well-known defective angiogenic behaviour. In addition, here we clearly demonstrate that a prolonged treatment with sera from SSc patients is capable of sustaining the EndoMT process in H-dMVECs. Of note, shorter time treatments with SSc sera have previously been shown to impair angiogenesis and survival of H-dMVECs [29,39,40]. Mechanistically, our present findings show that MMP-12-dependent cleavage of uPAR, a process which has been deeply implicated either in the impaired angiogenic performance of SSc-dMVECs or in fibroblast-to-myofibroblast differentiation [35,41,42], takes part in the pro-EndoMT effect exerted by SSc sera. Besides MMP-12, additional as yet unidentified circulating factors might trigger EndoMT and the loss of microvascular integrity in SSc dermis. Though further in-depth studies will be required, potential candidates include a large array of mediators which are elevated in SSc and have been demonstrated to induce EndoMT in vitro, such as TGFβ1, ET-1, tumour necrosis factor-α, asymmetric dimethylarginine and endostatin [16,19,26,48,49]. Consistent with our in vitro observations, a recent study reported that sera from patients with chronic kidney disease induced EndoMT, decreased proliferation and increased apoptosis of human coronary artery ECs [49]. These effects were mainly attributable to increased concentrations of circulating angiogenesis and nitric oxide inhibitors [49]. Finally, when considering the autoimmune background of SSc, we

cannot exclude the possible implication of functional (agonistic) autoantibodies against cell surface receptors in the EndoMT process. Indeed, a high proportion of SSc patients display agonistic autoantibodies against the angiotensin II type 1 receptor and the ET-1 type A receptor which can induce a variety of cellular responses such as production of TGFβ by dMVECs and synthesis of type I collagen by skin fibroblasts [50]. Further mechanistic studies aimed at identifying key initiators of EndoMT in SSc are warranted.

In summary, our data collectively support the notion that EndoMT is a process occurring in the dermal endothelium of SSc patients, where it may represent a crucial link between EC dysfunction and development of fibrosis. Hence, preventing or blocking EndoMT might be a novel and useful approach to treat peripheral microvasculopathy and prevent, at least in part, skin fibrosis in SSc patients.

Contributors

Study conception and design: MM, ER, LI-M and MM-C. Acquisition of data: MM, ER, IR, SG, SB-R, ADP, LI-M and MM-C. Interpretation of data: MM, ER, IR, LI-M and MM-C. Manuscript preparation: MM and MM-C.

Funding

Supported by grants from the University of Florence (Progetti di Ricerca di Ateneo to LI-M and MM-C).

Competing interests

None declared.

Ethics approval

The study was approved by the local institutional review board at the Azienda Ospedaliero-Universitaria Careggi (AOUC), Florence, Italy, and all subjects provided written informed consent.

REFERENCES

1. Allanore Y, Simms R, Distler O, *et al.* Systemic sclerosis. *Nat Rev Dis Primers* 2015;1:15002.
2. Gabrielli A, Avvedimento EV, Krieg T. Scleroderma. *N Engl J Med* 2009;360:1989-2003.
3. Matucci-Cerinic M, Kahaleh B, Wigley FM. Evidence that systemic sclerosis is a vascular disease. *Arthritis Rheum* 2013;65:1953-62.
4. Hinz B, Phan SH, Thannickal VJ, *et al.* Recent developments in myofibroblast biology: paradigms for connective tissue remodeling. *Am J Pathol* 2012;180:1340-55.
5. Hu B, Phan SH. Myofibroblasts. *Curr Opin Rheumatol* 2013;25:71-7.
6. Kis K, Liu X, Hagood JS. Myofibroblast differentiation and survival in fibrotic disease. *Expert Rev Mol Med* 2011;13:e27.
7. Hinz B. The extracellular matrix and transforming growth factor-β1: Tale of a strained relationship. *Matrix Biol* 2015;47:54-65.
8. Hinz B. The myofibroblast: paradigm for a mechanically active cell. *J Biomech* 2010;43:146-55.
9. Huang X, Yang N, Fiore VF, *et al.* Matrix stiffness-induced myofibroblast differentiation is mediated by intrinsic mechanotransduction. *Am J Respir Cell Mol Biol* 2012;47:340-8.
10. Gerber EE, Gallo EM, Fontana SC, *et al.* Integrin-modulating therapy prevents fibrosis and autoimmunity in mouse models of scleroderma. *Nature* 2013;503:126-30.
11. Hinz B, Phan SH, Thannickal VJ, *et al.* The myofibroblast: one function, multiple origins. *Am J Pathol* 2007;170:1807-16.
12. Ebmeier S, Horsley V. Origin of fibrosing cells in systemic sclerosis. *Curr Opin Rheumatol* 2015;27:555-62.
13. Marangoni RG, Korman BD, Wei J, *et al.* Myofibroblasts in murine cutaneous fibrosis originate from adiponectin-positive intradermal progenitors. *Arthritis Rheumatol* 2015;67:1062-73.
14. Piera-Velazquez S, Li Z, Jimenez SA. Role of endothelial-mesenchymal transition (EndoMT) in the pathogenesis of fibrotic disorders. *Am J Pathol* 2011;179:1074-80.
15. Manetti M, Guiducci S, Matucci-Cerinic M. The origin of the myofibroblast in fibroproliferative vasculopathy: does the endothelial cell steer the pathophysiology of systemic sclerosis? *Arthritis Rheum* 2011;63:2164-7.
16. Jimenez SA, Piera-Velazquez S. Endothelial to mesenchymal transition (EndoMT) in the pathogenesis of Systemic Sclerosis-associated pulmonary fibrosis and pulmonary arterial hypertension. Myth or reality? *Matrix Biol* 2016;51:26-36.

17. He J, Xu Y, Koya D, *et al.* Role of the endothelial-to-mesenchymal transition in renal fibrosis of chronic kidney disease. *Clin Exp Nephrol* 2013;17:488-97.
18. Li J, Bertram JF. Review: Endothelial-myofibroblast transition, a new player in diabetic renal fibrosis. *Nephrology (Carlton)* 2010;15:507-12.
19. Rieder F, Kessler SP, West GA, *et al.* Inflammation-induced endothelial-to-mesenchymal transition: a novel mechanism of intestinal fibrosis. *Am J Pathol* 2011;179:2660-73.
20. Kitao A, Sato Y, Sawada-Kitamura S, *et al.* Endothelial to mesenchymal transition via transforming growth factor-beta1/Smad activation is associated with portal venous stenosis in idiopathic portal hypertension. *Am J Pathol* 2009;175:616-26.
21. Ranchoux B, Antigny F, Rucker-Martin C, *et al.* Endothelial-to-mesenchymal transition in pulmonary hypertension. *Circulation* 2015;131:1006-18.
22. Arciniegas E, Sutton AB, Allen TD, *et al.* Transforming growth factor beta 1 promotes the differentiation of endothelial cells into smooth muscle-like cells in vitro. *J Cell Sci* 1992;103:521-9.
23. Zeisberg EM, Potenta SE, Sugimoto H, *et al.* Fibroblasts in kidney fibrosis emerge via endothelial-to-mesenchymal transition. *J Am Soc Nephrol* 2008;19:2282-7.
24. Li Z, Jimenez SA. Protein kinase Cδ and c-Abl kinase are required for transforming growth factor β induction of endothelial-mesenchymal transition in vitro. *Arthritis Rheum* 2011;63:2473-83.
25. Mendoza FA, Piera-Velazquez S, Farber JL, *et al.* Endothelial cells expressing endothelial and mesenchymal cell gene products in lung tissue from patients with systemic sclerosis-associated interstitial lung disease. *Arthritis Rheumatol* 2016;68:210-7.
26. Good RB, Gilbane AJ, Trinder SL, *et al.* Endothelial to mesenchymal transition contributes to endothelial dysfunction in pulmonary arterial hypertension. *Am J Pathol* 2015;185:1850-8.
27. van den Hoogen F, Khanna D, Fransen J, *et al.* 2013 classification criteria for systemic sclerosis: an American college of rheumatology/European league against rheumatism collaborative initiative. *Ann Rheum Dis* 2013;72:1747-55.
28. Manetti M, Guiducci S, Romano E, *et al.* Overexpression of VEGF165b, an inhibitory splice variant of vascular endothelial growth factor, leads to insufficient angiogenesis in patients with systemic sclerosis. *Circ Res* 2011;109:e14-26.
29. Romano E, Chora I, Manetti M, *et al.* Decreased expression of neuropilin-1 as a novel key factor contributing to peripheral microvasculopathy and defective angiogenesis in systemic sclerosis. *Ann Rheum Dis* 2016;75:1541-9.

30. Manetti M, Guiducci S, Romano E, *et al.* Decreased expression of the endothelial cell-derived factor EGFL7 in systemic sclerosis: potential contribution to impaired angiogenesis and vasculogenesis. *Arthritis Res Ther* 2013;15:R165.
31. Distler JH, Jüngel A, Huber LC, *et al.* Imatinib mesylate reduces production of extracellular matrix and prevents development of experimental dermal fibrosis. *Arthritis Rheum* 2007;56:311-22.
32. Manetti M, Rosa I, Milia AF, *et al.* Inactivation of urokinase-type plasminogen activator receptor (uPAR) gene induces dermal and pulmonary fibrosis and peripheral microvasculopathy in mice: a new model of experimental scleroderma? *Ann Rheum Dis* 2014;73:1700-9.
33. Manetti M, Rosa I, Fazi M, *et al.* Systemic sclerosis-like histopathological features in the myocardium of uPAR-deficient mice. *Ann Rheum Dis* 2016;75:474-8.
34. Manetti M, Guiducci S, Ruffo M, *et al.* Evidence for progressive reduction and loss of telocytes in the dermal cellular network of systemic sclerosis. *J Cell Mol Med* 2013;17:482-96.
35. Margheri F, Manetti M, Serrati S, *et al.* Domain 1 of the urokinase-type plasminogen activator receptor is required for its morphologic and functional, beta2 integrin-mediated connection with actin cytoskeleton in human microvascular endothelial cells: failure of association in systemic sclerosis endothelial cells. *Arthritis Rheum* 2006;54:3926-38.
36. Asano Y, Stawski L, Hant F, *et al.* Endothelial Fli1 deficiency impairs vascular homeostasis: a role in scleroderma vasculopathy. *Am J Pathol* 2010;176:1983-98.
37. Taniguchi T, Asano Y, Akamata K, *et al.* Fibrosis, vascular activation, and immune abnormalities resembling systemic sclerosis in bleomycin-treated Fli-1-haploinsufficient mice. *Arthritis Rheumatol* 2015;67:517-26.
38. Manetti M. Fli1 deficiency and beyond: a unique pathway linking peripheral vasculopathy and dermal fibrosis in systemic sclerosis. *Exp Dermatol* 2015;24:256-7.
39. Romano E, Bellando-Randone S, Manetti M, *et al.* Bosentan blocks the antiangiogenic effects of sera from systemic sclerosis patients: an in vitro study. *Clin Exp Rheumatol* 2015;33(4 Suppl 91):S148-52.
40. Borghini A, Manetti M, Nacci F, *et al.* Systemic sclerosis sera impair angiogenic performance of dermal microvascular endothelial cells: therapeutic implications of cyclophosphamide. *PLoS One* 2015;10:e0130166.
41. Manetti M, Guiducci S, Ibba-Manneschi L, *et al.* Mechanisms in the loss of capillaries in systemic sclerosis: angiogenesis versus vasculogenesis. *J Cell Mol Med* 2010;14:1241-54.

42. Bernstein AM, Twining SS, Warejcka DJ, *et al.* Urokinase receptor cleavage: a crucial step in fibroblast-to-myofibroblast differentiation. *Mol Biol Cell* 2007;18:2716-27.
43. Manetti M, Guiducci S, Romano E, *et al.* Increased serum levels and tissue expression of matrix metalloproteinase-12 in patients with systemic sclerosis: correlation with severity of skin and pulmonary fibrosis and vascular damage. *Ann Rheum Dis* 2012;71:1064-72.
44. Hashimoto N, Phan SH, Imaizumi K, *et al.* Endothelial-mesenchymal transition in bleomycin-induced pulmonary fibrosis. *Am J Respir Cell Mol Biol* 2010;43:161-72.
45. Zeisberg EM, Tarnavski O, Zeisberg M, *et al.* Endothelial-to-mesenchymal transition contributes to cardiac fibrosis. *Nat Med* 2007;13:952-61.
46. Tsou PS, Rabquer BJ, Ohara RA, *et al.* Scleroderma dermal microvascular endothelial cells exhibit defective response to pro-angiogenic chemokines. *Rheumatology (Oxford)* 2016;55:745-54.
47. Giusti B, Fibbi G, Margheri F, *et al.* A model of anti-angiogenesis: differential transcriptosome profiling of microvascular endothelial cells from diffuse systemic sclerosis patients. *Arthritis Res Ther* 2006;8:R115.
48. Wermuth PJ, Li Z, Mendoza FA, *et al.* Stimulation of transforming growth factor-β1-induced endothelial-to-mesenchymal transition and tissue fibrosis by endothelin-1 (ET-1): a novel profibrotic effect of ET-1. *PLoS One* 2016;11:e0161988.
49. Charytan DM, Padera R, Helfand AM, *et al.* Increased concentration of circulating angiogenesis and nitric oxide inhibitors induces endothelial to mesenchymal transition and myocardial fibrosis in patients with chronic kidney disease. *Int J Cardiol* 2014;176:99-109.
50. Cabral-Marques O, Riemekasten G. Vascular hypothesis revisited: Role of stimulating antibodies against angiotensin and endothelin receptors in the pathogenesis of systemic sclerosis. *Autoimmun Rev* 2016;15:690-4.

FIGURE LEGENDS

Figure 1. Detection of endothelial-to-mesenchymal transition (EndoMT) in dermal vessels of patients with systemic sclerosis (SSc). (A) Representative fluorescence microphotographs of skin sections from healthy controls and patients with SSc double immunostained for the endothelial cell (EC) markers CD31 or VE-cadherin (red) and the myofibroblast marker α-smooth muscle actin (α-SMA; green) and counterstained with 4',6-diamidino-2-phenylindole (DAPI; blue) for nuclei. In healthy dermal vessels, α-SMA expression is mostly restricted to pericytes and vascular smooth muscle cells surrounding ECs. In SSc skin, colocalised CD31/α-SMA and VE-cadherin/α-SMA give rise to yellow staining which is evident in transitional EndoMT cells of numerous capillary vessels (arrows) and arterioles (arrowheads). In each panel, insets show higher magnification views of dermal microvessels. Scale bar=50 μm. (B) The percentage of dermal vessels displaying CD31/α-SMA and VE-cadherin/α-SMA colocalisation is significantly increased in skin biopsies from SSc patients (n=12) compared with healthy skin (n=10). Data are mean±SEM. *$p<0.001$ versus healthy skin. (C) Representative transmission electron microscopy microphotographs of dermal capillary vessels from healthy controls (n=5) and patients with SSc (n=5). At least eight capillary vessels from each of three ultrathin sections per sample were analysed. Numerous Weibel-Palade bodies (arrows) are present in healthy dermal ECs, while they are reduced or even absent in SSc dermal ECs. Scale bar=2 μm.

Figure 2. Detection of endothelial-to-mesenchymal transition (EndoMT) in dermal vessels of murine models of systemic sclerosis (SSc). (A and B) Representative fluorescence microphotographs of mouse skin sections double immunostained for either CD31 (red) (A) or VE-cadherin (red) (B) endothelial cell markers and the myofibroblast marker α-smooth muscle actin (α-SMA; green) with 4',6-diamidino-2-phenylindole (DAPI; blue) counterstain for nuclei are shown. In the dermis of bleomycin-treated mice and urokinase-type plasminogen activator receptor (uPAR)-deficient mice, colocalisation of either CD31 or VE-cadherin and α-SMA gives rise to yellow staining which is evident in transitional EndoMT cells of numerous microvessels (arrows). Insets show higher magnification views of dermal microvessels from the corresponding panels. Scale bar=50 μm. The percentage of dermal vessels displaying CD31/α-SMA or VE-cadherin/α-SMA colocalisation is reported in the histograms. Data are mean±SEM (6 mice in each experimental group). *$p<0.001$ versus saline-treated mice (A and B, top), *$p<0.001$ versus wild-type littermates (A and B, bottom).

Figure 3. Dermal microvascular endothelial cells (dMVECs) isolated from systemic sclerosis (SSc) skin coexpress endothelial and mesenchymal cell markers and exhibit a myofibroblast-like functional phenotype. (A) Representative fluorescence microphotographs of healthy dMVECs (H-dMVECs) and SSc-dMVECs (n=6 each) immunostained for CD31, VE-cadherin, α-smooth muscle actin (α-SMA), F-actin (phalloidin), S100A4/fibroblast-specific protein-1 (FSP1), type I collagen and Snail1 transcription factor. Nuclei are counterstained with 4',6-diamidino-2-phenylindole (DAPI). Both H-dMVECs and SSc-dMVECs are immunopositive for the pan-endothelial cell marker CD31. The expression of CD31 and VE-cadherin is markedly lower in SSc-dMVECs compared with H-dMVECs. SSc-dMVECs exhibit α-SMA+ stress fibres (shown at higher magnification in the inset), a marked increase in phalloidin+ stress fibres mainly organised longitudinally, and expression of S100A4/FSP1, type I collagen and nuclear Snail1. In H-dMVECs, α-SMA and type I collagen are undetectable, while expression of S100A4/FSP1 and Snail1 is negligible. Scale bar=50 μm. (B) Representative fluorescence microphotographs of SSc-dMVECs double immunostained for CD31 (red) and α-SMA (green) with DAPI (blue) counterstain for nuclei. Note the presence of CD31+ cells displaying α-SMA+ stress fibres. Cells labelled as (1) and (2) in the left panel are shown at higher magnification in the right panels. The degree of α-SMA arrangement into stress fibres varies among cells. Scale bar=50 μm (left panel), 20 μm (right

panels). The percentage of CD31/α-SMA double-positive cells is reported in the histograms. Data are mean±SEM. *p<0.001 versus H-dMVECs. (C) Protein lysates from H-dMVECs and SSc-dMVECs were assayed for the expression of CD31, VE-cadherin, α-SMA, S100A4/FSP1, type I collagen, Snail1 and Friend leukemia integration-1 (Fli1). Representative immunoblots are shown. Molecular weight values (kDa) are indicated. The densitometric analysis of the bands normalised to α-tubulin is reported in the histograms. Data are mean±SEM of optical density in arbitrary units (a.u.). *p<0.001 versus H-dMVECs. Results are representative of three independent experiments performed with each of the six H-dMVEC and SSc-dMVEC lines. (D) Collagen gel contraction assay with H-dMVECs and SSc-dMVECs (n=6 each). Gel size in the presence of SSc-dMVECs is expressed as percentage of that observed in the presence of H-dMVECs. Data are mean±SEM. *p<0.001 versus H-dMVECs.

Figure 4. Treatment with sera from patients with systemic sclerosis (SSc) induces a myofibroblast-like morphology and functional phenotype in healthy dermal microvascular endothelial cells (H-dMVECs). (A) Representative phase-contrast microphotographs of H-dMVECs (n=3) at baseline and after treatment for 48 and 72 hours (h) with sera from healthy subjects (n=6), sera from patients with SSc (n=6) or recombinant human transforming growth factor-β1 (rh TGFβ1; 10 ng/ml) are shown (x10 original magnification). The morphology of H-dMVECs does not change over time in cultures treated with healthy sera. After 48-hour treatment either with SSc sera or rh TGFβ1, H-dMVECs start to disaggregate and lose their characteristic polygonal cobblestone-like morphology. Cells exhibiting a spindle-shaped morphology are clearly veasible in H-dMVEC cultures treated either with SSc sera or rh TGFβ1 for 72 hours. The percentage of spindle-shaped cells is reported in the histograms. Data are mean±SEM. *p<0.001 versus basal H-dMVECs. (B) Collagen gel contraction assay with H-dMVECs at baseline and after treatment for 72 h with healthy sera (n=6), SSc sera (n=6) or rh TGFβ1. Gel size in the different experimental conditions is expressed as percentage of baseline. Data are mean±SEM. *p<0.001 versus basal H-dMVECs.

Figure 5. Treatment with sera from patients with systemic sclerosis (SSc) induces changes in mRNA expression levels of endothelial and mesenchymal cell markers in healthy dermal microvascular endothelial cells (H-dMVECs). H-dMVECs were treated for 48 hours with sera from healthy subjects (n=6), sera from patients with SSc (n=6) or recombinant human transforming growth factor-β1 (TGFβ1; 10 ng/ml) and subsequently assayed for mRNA expression levels of *CD31*, *CDH5* (VE-cadherin), *FLI1*, *ACTA2* (α-SMA), *S100A4*, *SNAI1* (Snail1), *COL1A1* and *COL1A2* genes by quantitative real-time PCR. Ribosomal protein S18 (*RPS18*) mRNA was measured as an endogenous control for normalisation. The relative values compared with basal H-dMVECs are expressed as mean±SEM of three independent experiments performed with three H-dMVEC lines. *p<0.001 versus basal H-dMVECs.

Figure 6. Treatment with sera from patients with systemic sclerosis (SSc) induces changes in protein expression levels of endothelial and mesenchymal cell markers in healthy dermal microvascular endothelial cells (H-dMVECs). H-dMVECs were treated for 72 hours with sera from healthy subjects (n=6), sera from patients with SSc (n=6) or recombinant human transforming growth factor-β1 (TGFβ1; 10 ng/ml) and subsequently assayed for protein expression levels of CD31, VE-cadherin, Friend leukemia integration-1 (Fli1), α-smooth muscle actin (α-SMA), S100A4/fibroblast-specific protein-1 (FSP1), Snail1 and type I collagen. (A) Representative immunoblots are shown. Molecular weight values (kDa) are indicated. Protein expression of α-tubulin was measured as a loading control. Results are representative of three independent experiments performed with three H-dMVEC lines. (B-D) Representative fluorescence microphotographs show H-dMVECs double immunostained for the endothelial cell marker CD31 (red) and the myofibroblast marker α-SMA (green), or immunostained for Snail1 (red) and type I collagen (red). Nuclei are counterstained with 4',6-diamidino-2-phenylindole (DAPI; blue).

Treatment of H-dMVECs either with SSc sera or TGFβ1, but not with healthy sera, induces downregulation of CD31 in parallel with the appearance of α-SMA+ stress fibres, strong expression and nuclear localisation of Snail1 and de novo synthesis of type I collagen. Scale bar=20 μm. (E-G) The percentage of CD31/α-SMA double-positive cells (E), Snail1+ nuclei (F) and type I collagen+ cells (G) is reported in the histograms. Data are mean±SEM. *p<0.001 versus basal H-dMVECs.

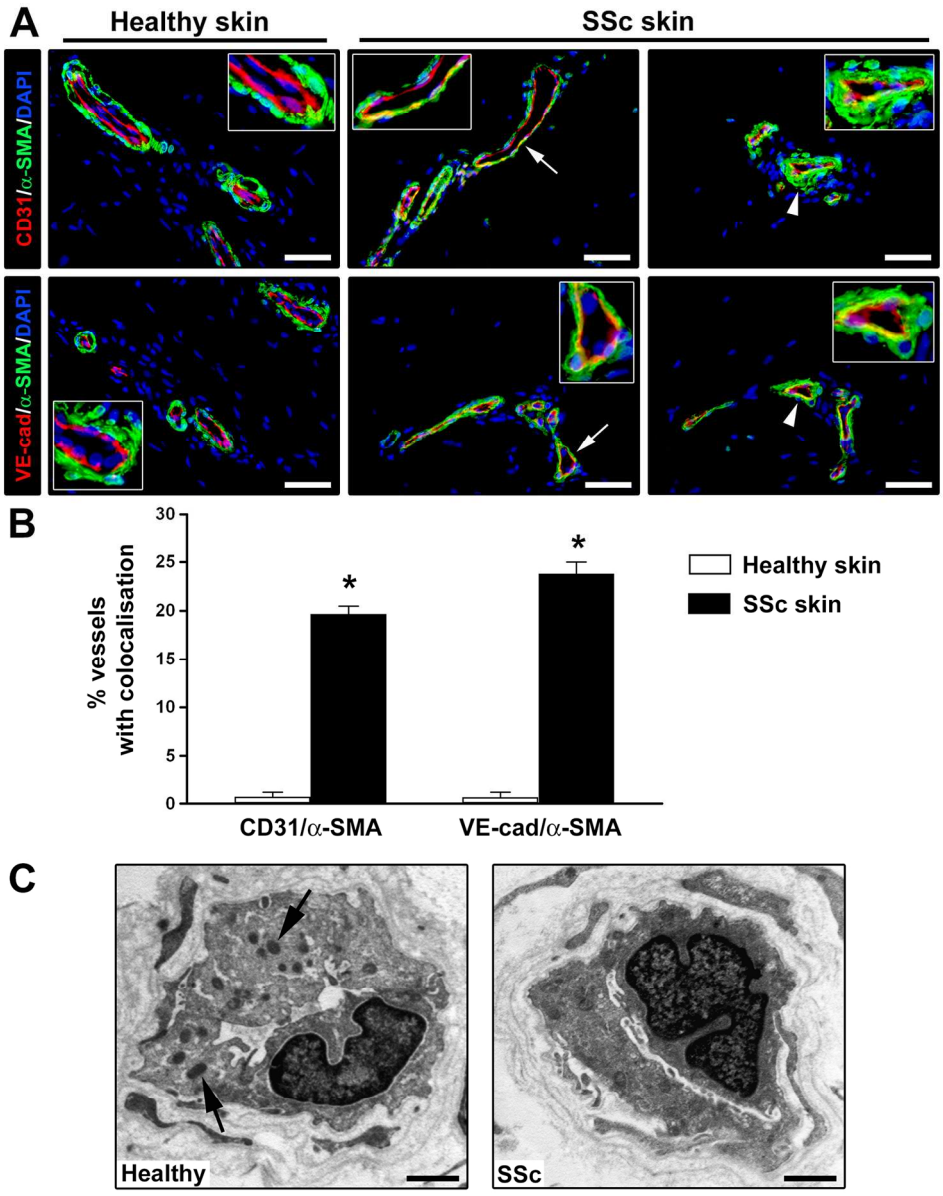

Figure 1

150x190mm (300 x 300 DPI)

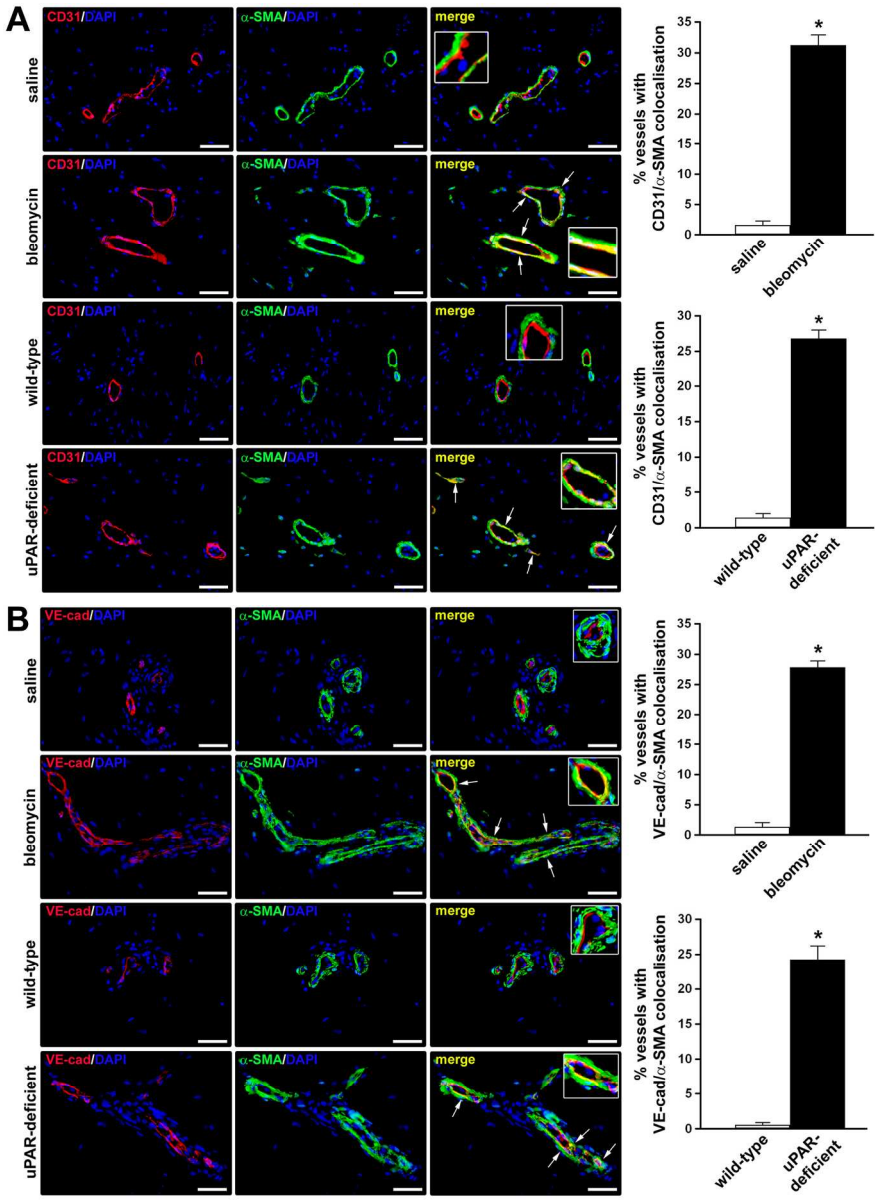

Figure 2

170x231mm (300 x 300 DPI)

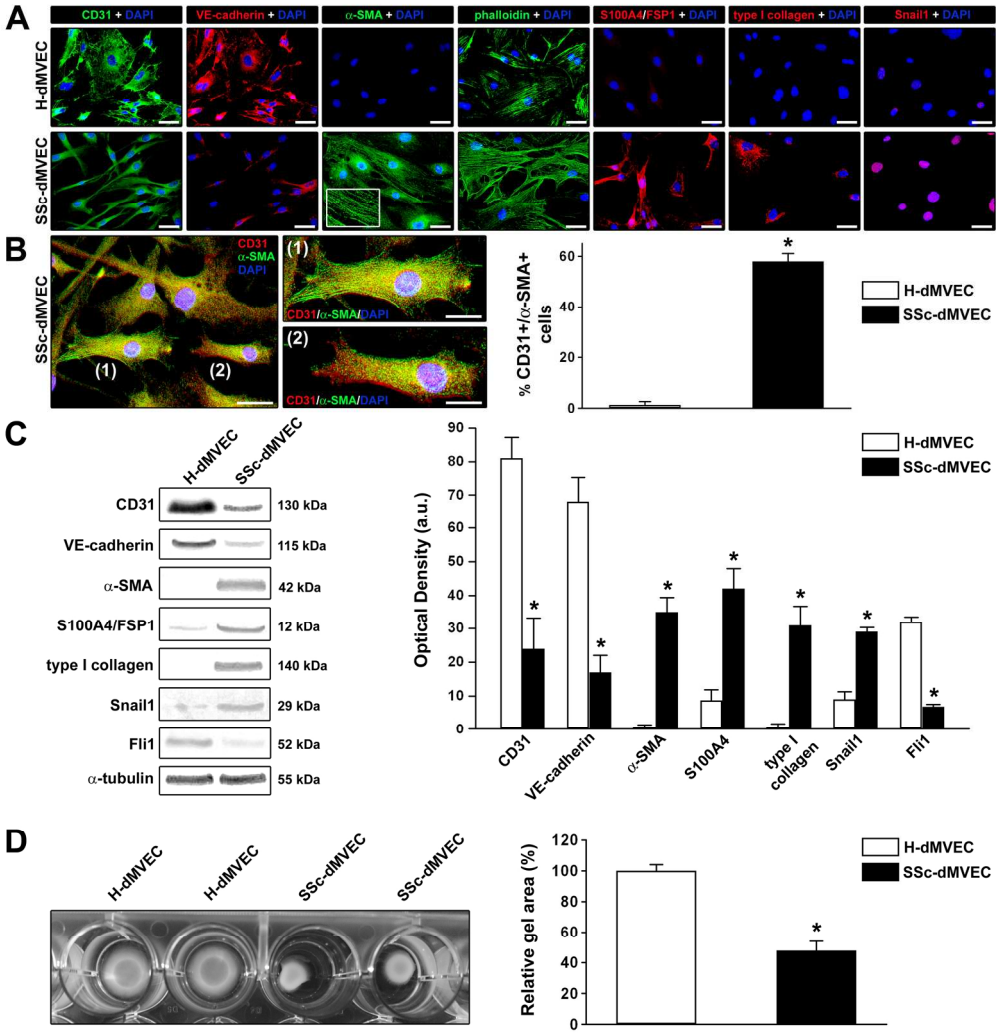

Figure 3

180x187mm (300 x 300 DPI)

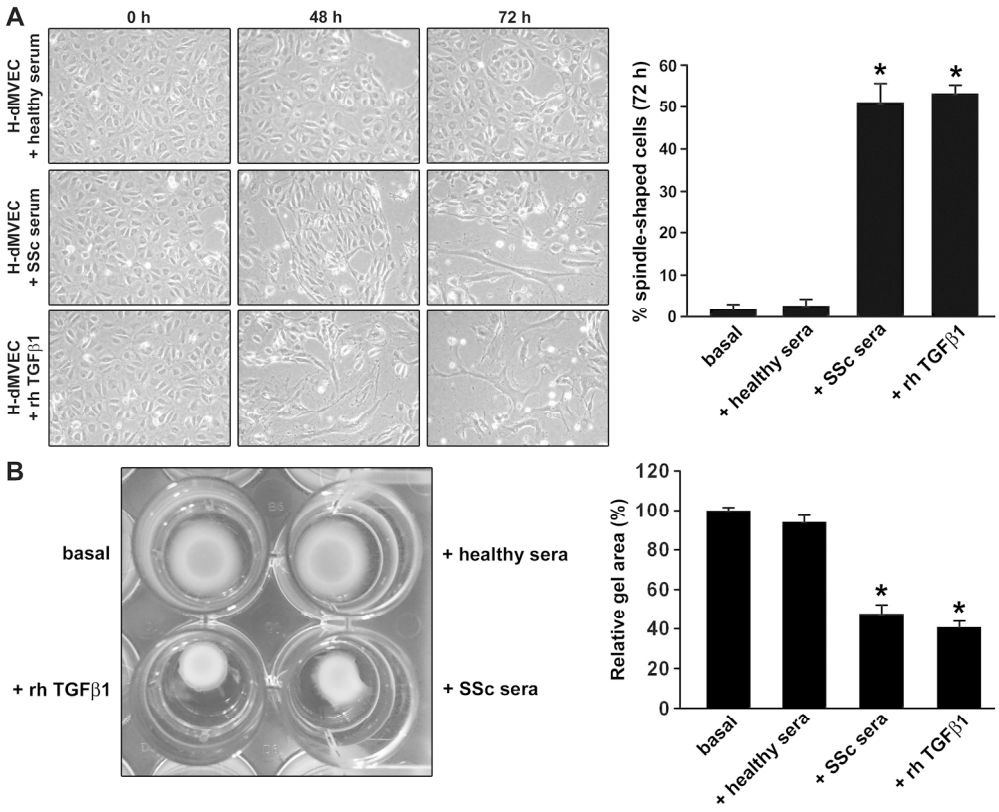

Figure 4

180x147mm (300 x 300 DPI)

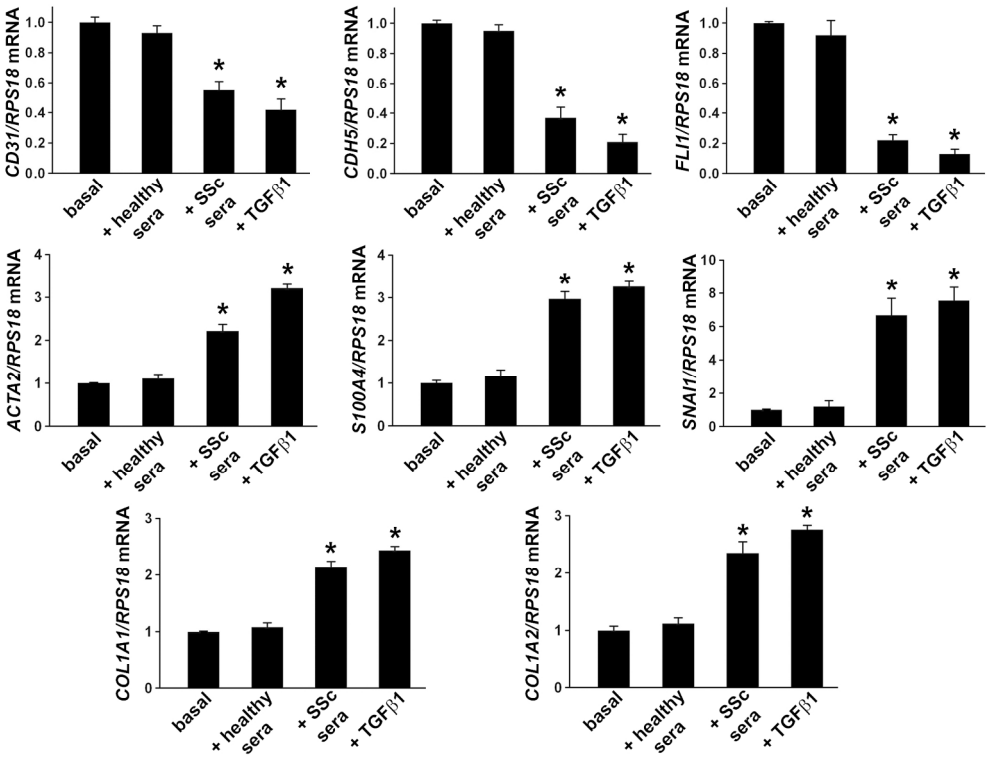

Figure 5

180x138mm (300 x 300 DPI)

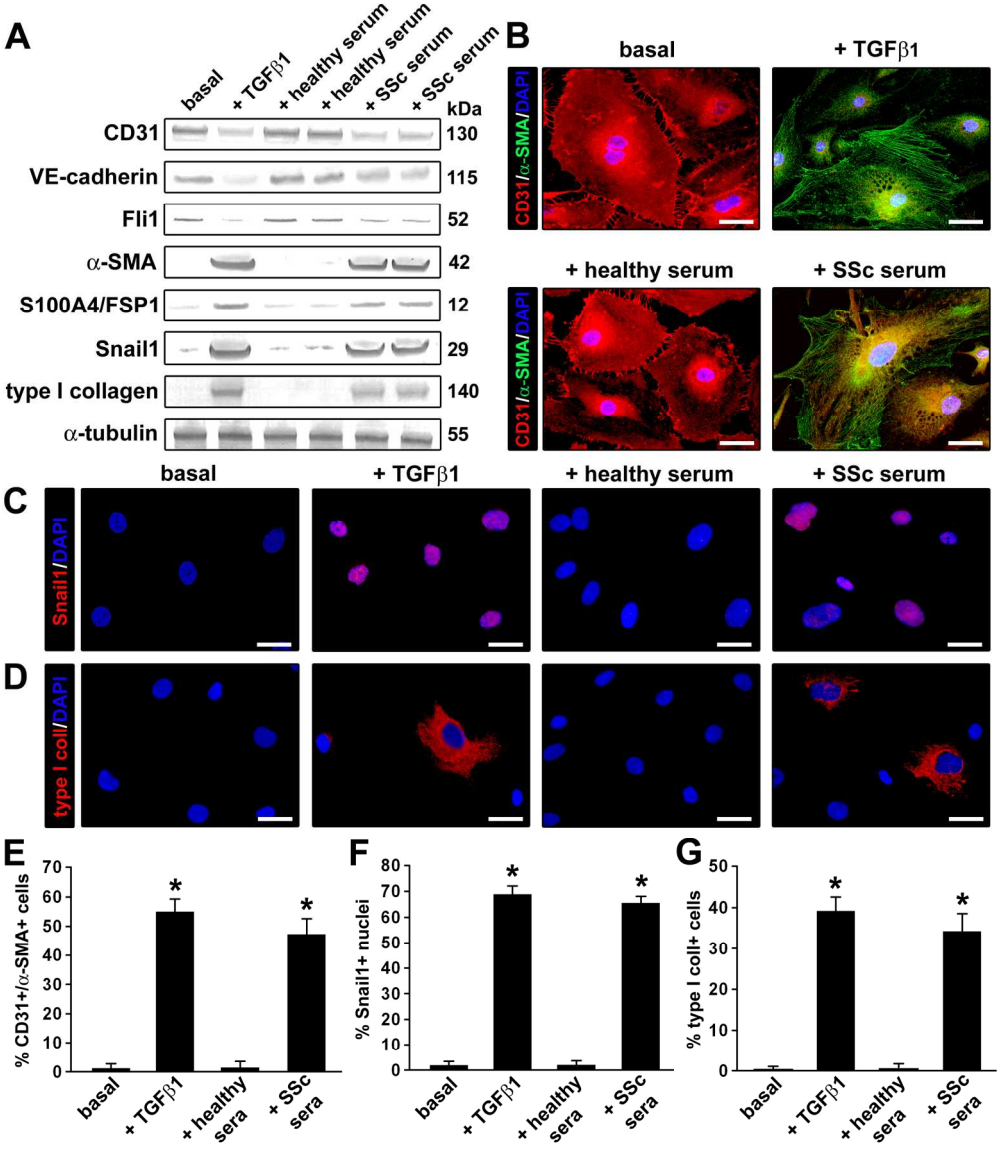

Figure 6

180x208mm (300 x 300 DPI)

ONLINE SUPPLEMENTARY MATERIAL

Manetti M, *et al.* **"Endothelial-to-mesenchymal transition contributes to endothelial dysfunction and dermal fibrosis in systemic sclerosis"**

MATERIALS AND METHODS

Cell culture and reagents

Primary cultures of dermal microvascular endothelial cells (dMVECs) were established by explantation from biopsies of the lesional forearm skin from 6 patients with early diffuse cutaneous systemic sclerosis (dcSSc; disease duration <2 years from first non-Raynaud symptom) [1] and from 6 healthy age-matched and gender-matched adult subjects under protocols approved by the Institutional Review Board of the Azienda Ospedaliero-Universitaria Careggi (AOUC), Florence, Italy, as described elsewhere [2,3]. At the time of biopsy, patients were not on immunosuppressive or disease-modifying drugs. Patient characteristics are summarised in online supplementary table S1. Skin biopsies were mechanically cleaned of epidermis and adipose tissue in order to obtain a pure specimen of vascularised dermis, and were processed as previously described [2,3]. Adherent cells were detached and subjected to CD31 immunomagnetic isolation by incubation with anti-CD31 conjugated-microbeads [2,3]. Isolated cells were further identified as endothelial cells by labelling with anti-factor VIII-related antigen (von Willebrand factor) and anti-CD105, followed by reprobing with anti-CD31 antibodies (see online supplementary figure S1). dMVECs from healthy subjects (H-dMVECs) and SSc patients (SSc-dMVECs) were maintained in MCDB 131 medium (Sigma-Aldrich, St. Louis, MO, USA) supplemented with 30% fetal bovine serum (FBS), 20 μg/ml endothelial cell growth supplement (Calbiochem, Nottingham, UK), 10 μg/ml hydrocortisone, 15 IU/ml heparin, and antibiotics in a humidified atmosphere of 5% CO_2 at 37°C, and used between the third and seventh passages in culture. In selected experiments, H-dMVECs were grown to confluence, and then were washed three times with serum-free medium and serum-starved overnight in MCDB 131 medium supplemented with 2% FBS. Medium was subsequently removed and cells were incubated with MCDB 131 medium containing 2% FBS and recombinant human transforming growth factor-β1 (TGFβ1) (10 ng/ml; PeproTech, Rocky Hill, NJ, USA) or 10% serum from early dcSSc patients (n=6) and healthy subjects (n=6) for 24, 48 and 72 hours. Each serum sample was tested individually. The medium was changed and additives replenished every day. In some experimental points, sera were preincubated with the matrix metalloproteinase-12 (MMP-12) specific inhibitor MMP408 (10 nM; Sigma-Aldrich) before cell stimulation. Phase-contrast images were obtained under a Leica inverted microscope (Leica Microsystems, Mannheim,

Germany) to assess cell morphology. The proportion of spindle-shaped cells relative to polygonal-shaped endothelial cells was assessed in at least ten randomly selected fields (x10 original magnification) per sample employing the ImageJ software (NIH, Bethesda, MD, USA). Cells with a diameter at their longest axis that was two-fold greater than the average diameter of untreated cobblestone H-dMVECs were considered spindle-shaped.

Fluorescence immunocytochemistry

H-dMVECs and SSc-dMVECs were seeded onto glass coverslips. In some experiments, H-dMVECs were treated as described above for 72 hours. At the end of the experiments, cells were fixed with 3.7% buffered paraformaldehyde and permeabilised with 0.1% Triton X-100 in phosphate buffered saline (PBS). Slides were washed with PBS and blocked with 1% bovine serum albumin in PBS for 1 hour at room temperature, and were then incubated overnight at 4°C with primary antibodies against CD31 (catalogue number ab9498; Abcam, Cambridge, UK) at 1:50 dilution, vascular endothelial (VE)-cadherin (catalogue number ab33168; Abcam) at 1:50 dilution, α-smooth muscle actin (α-SMA) (catalogue number ab7817; Abcam) at 1:100 dilution, S100A4/fibroblast-specific protein-1 (FSP1) (catalogue number ab124805; Abcam) at 1:100 dilution, type I collagen (catalogue number ab90395; Abcam) at 1:100 dilution, or Snail1 (catalogue number ab167609; Abcam) at 1:50 dilution, followed by incubation for 45 minutes at room temperature in the dark with Alexa Fluor-488-conjugated or Rhodamine Red-X-conjugated secondary antibodies at 1:200 dilution (Invitrogen, Carlsbad, CA, USA). Double immunofluorescence staining was performed by mixing mouse anti-α-SMA (1:100 dilution; catalogue number ab7817; Abcam) and rabbit anti-CD31 (1:20 dilution; catalogue number ab28364; Abcam) primary antibodies and subsequently mixing fluorochrome-conjugated secondary antibodies. Irrelevant isotype-matched and concentration-matched mouse and rabbit IgG (Sigma-Aldrich) were used as negative controls. In some specimens, Alexa 488-labelled phalloidin (1:40 dilution; Invitrogen) was applied to the cells to visualise the arrangement of the F-actin cytoskeleton. Nuclei were counterstained with 4′,6-diamidino-2-phenylindole (DAPI). Immunolabelled cells were examined with a Leica DM4000 B microscope (Leica Microsystems) and fluorescence images were captured with a Leica DFC310 FX 1.4-megapixel digital colour camera equipped with the Leica software application suite LAS V3.8 (Leica Microsystems).

RNA isolation and quantitative real-time PCR

At the end of the experiments, cultures were harvested, and total RNA was isolated using the RNeasy Micro Kit (Qiagen, Milan, Italy). First strand cDNA synthesis and mRNA quantification by

SYBR Green real-time PCR using the StepOnePlus Real-Time PCR System (Applied Biosystems, Milan, Italy) were performed as reported elsewhere [3]. Predesigned oligonucleotide primer pairs were obtained from Qiagen (QuantiTect Primer Assay). The assay IDs were Hs_PECAM1_1_SG (CD31; catalogue number QT00081172), Hs_CDH5_1_SG (VE-cadherin; catalogue number QT00013244), Hs_ACTA2_1_SG (α-SMA; catalogue number QT00088102), Hs_S100A4_1_SG (catalogue number QT00014259), Hs_COL1A1_1_SG (catalogue number QT00037793), Hs_COL1A2_1_SG (catalogue number QT00072058), Hs_SNAI1_1_SG (Snail1; catalogue number QT00010010), Hs_FLI1_1_SG (catalogue number QT00078372), and Hs_RPS18_1_SG (catalogue number QT00248682). Ribosomal protein S18 (RPS18) mRNA was measured as an endogenous control to normalise for the amounts of loaded cDNA. Differences were calculated with the threshold cycle (Ct) and comparative Ct method for relative quantification. All measurements were performed in triplicate.

Immunoblotting

Whole cell protein lysates from dMVECs were subjected to immunoblot analysis as described elsewhere [3]. The following antibodies were used at 1:1000 dilution: anti-CD31 (catalogue number ab9498; Abcam), anti-VE-cadherin (catalogue number ab33168; Abcam), anti-α-SMA (catalogue number ab7817; Abcam), anti-S100A4/FSP1 (catalogue number ab124805; Abcam), anti-type I collagen (catalogue number ab90395; Abcam), anti-Snail1 (catalogue number ab167609; Abcam), anti-Friend leukemia integration-1 (Fli1) (catalogue number ab180902; Abcam), and anti-α-tubulin (catalogue number #2144; Cell Signaling Technology, Danvers, MA, USA). Anti-urokinase-type plasminogen activator receptor (uPAR) domain 1 (D1) (catalogue number 3931; American Diagnostica, Stamford, CT, USA) and anti-uPAR domain 2 (D2) (catalogue number 3932; American Diagnostica) antibodies were used at 1:200 dilution. Immunodetection was performed using the Western Breeze Chromogenic Western Blot Immunodetection Kit (Invitrogen). Band intensities were quantified with the ImageJ software (NIH) and normalised with α-tubulin in each sample.

Collagen gel contraction assay

Collagen gel contraction assays were performed using the CytoSelect™ 24-Well Cell Contraction Assay Kit (Floating Matrix Model; catalogue number CBA-5020; Cell Biolabs, San Diego, CA, USA) according to the manufacturer's instructions. H-dMVECs and SSc-dMVECs were harvested, pelleted and resuspended in serum-free medium at 5×10^6 cells/ml. In some experimental points, H-dMVECs were treated with recombinant human TGFβ1 (10 ng/ml; PeproTech) or 10% serum from

early dcSSc patients (n=6) and healthy subjects (n=6) for 72 hours before the assays. For each assay, 100 µl of the cell suspension was mixed with 400 µl of cold neutralised collagen gel solution and subsequently added to one well of the adhesion resistant matrix-coated 24-well cell contraction plate. Gels were allowed to solidify for 1 hour at 37°C and 5% CO_2. After polymerisation, 1 ml of basal media or media containing different stimuli (i.e. TGFβ1, early dcSSc sera and healthy sera) was added to the top of each collagen gel lattice. Gels without cells were included as negative controls. Each experimental point was performed in triplicate. After 24 hours, the culture dish was scanned and the area of each collagen gel was measured by ImageJ software (NIH).

Enzyme-linked immunosorbent assay

Levels of MMP-12 in serum samples were measured by commercial quantitative colorimetric sandwich enzyme-linked immunosorbent assay (Human Matrix Metallopeptidase 12 ELISA Kit; Antibodies-online, Atlanta, GA, USA) according to the manufacturer's protocol. The detection range was 0.156-10 ng/ml. Concentrations were calculated using a standard curve generated with specific standards provided by the manufacturer. Each sample was measured in duplicate.

Fluorescence immunohistochemistry on human and mouse skin

To assess the presence of endothelial-to-mesenchymal transition (EndoMT) in the skin, paraffin-embedded sections of lesional forearm skin biopsies were obtained from 12 SSc patients (10 women and 2 men; n=4 with limited cutaneous SSc and n=8 with dcSSc) [1] and 10 age- and sex-matched healthy donors, as described elsewhere [2,3]. Biopsies were obtained under protocols approved by the Institutional Review Board of the AOUC, Florence, Italy. After antigen retrieval, quenching of autofluorescence and blocking of nonspecific binding sites [4], skin sections (5 µm thick) were examined by double-label immunofluorescence using antibodies against α-SMA (1:50 dilution; catalogue number ab7817; Abcam) and CD31 (1:50 dilution; catalogue number ab28364; Abcam) or VE-cadherin (1:50 dilution; catalogue number ab33168; Abcam), followed by fluorochrome-conjugated secondary antibodies (Invitrogen) as well as DAPI to identify nuclei. Negative controls stained without primary antibody were used to confirm specificity. Images were acquired on a Leica DM4000 B microscope (Leica Microsystems) equipped with a Leica DFC310 FX 1.4-megapixel digital colour camera and the Leica software application suite LAS V3.8 (Leica Microsystems). The percentage of dermal vessels displaying CD31/α-SMA and VE-cadherin/α-SMA colocalisation was determined in five randomly selected high-power fields (hpf; x40 original magnification) of the dermis from each of three sections per sample by two independent blinded observers. To examine the presence of EndoMT in vivo, skin sections from two mouse models of dermal fibrosis were

used. First, 6 week-old male C57BL/6 mice (Charles River Laboratories, Calco, Lecco, Italy) received subcutaneous injections of 100 µl of bleomycin dissolved in 0.9% NaCl (saline solution) at a concentration of 0.5 mg/ml every other day for 4 weeks in well-defined areas (1 cm^2) of the upper back. Subcutaneous injections of 0.9% NaCl served as controls [5]. The second model consisted of 12 week-old male uPAR-deficient mice and wild-type littermates as described elsewhere [6,7]. All animal protocols were performed in accordance with DL 116/92 and approved by the Institutional Animal Care and Use Committee of the University of Florence. Each experimental group consisted of at least six mice. At the end of the experiments, mice were anesthetised intraperitoneally with cloralium hydrate (400 mg/kg) and sacrificed by cervical dislocation. Lesional skin was harvested, and double immunofluorescence using antibodies against α-SMA (1:50 dilution; catalogue number ab7817; Abcam) and CD31 (1:50 dilution; catalogue number ab28364; Abcam) or VE-cadherin (1:50 dilution; catalogue number ab33168; Abcam), followed by incubation with Alexa Fluor-488-conjugated and Rhodamine Red-X-conjugated IgG (Invitrogen) and DAPI, was performed. Irrelevant IgG were used as negative controls. Sections were imaged at x40 original magnification at five randomly selected hpf spanning the dermis under a Leica DM4000 B microscope (Leica Microsystems). The proportion of vessels with CD31/α-SMA and VE-cadherin/α-SMA colocalisation was scored in at least five hpf of the dermis from each of three sections per mouse by two independent blinded observers.

Transmission electron microscopy

Ultrathin sections (~70 nm thick) from skin biopsies from 5 dcSSc patients and 5 healthy controls were examined and photographed under a JEOL JEM-1010 electron microscope (Jeol, Tokyo, Japan) equipped with a MegaView III high-resolution digital camera and imaging software (Jeol), as described elsewhere [8]. At least eight capillary vessels from each of three ultrathin sections per sample were analysed.

Statistical analysis

Statistical analyses were performed using the Statistical Package for Social Sciences (SPSS) software for Windows, V.20.0 (SPSS, Chicago, IL, USA). Data are expressed as means and standard errors of the mean (SEM). The Student's t-test was used for statistical evaluation of the differences between two independent groups. A p value of <0.05 according to a two-tailed distribution was considered statistically significant.

REFERENCES

1. van den Hoogen F, Khanna D, Fransen J, *et al.* 2013 classification criteria for systemic sclerosis: an American college of rheumatology/European league against rheumatism collaborative initiative. *Ann Rheum Dis* 2013;72:1747-55.
2. Manetti M, Guiducci S, Romano E, *et al.* Overexpression of VEGF165b, an inhibitory splice variant of vascular endothelial growth factor, leads to insufficient angiogenesis in patients with systemic sclerosis. *Circ Res* 2011;109:e14-26.
3. Romano E, Chora I, Manetti M, *et al.* Decreased expression of neuropilin-1 as a novel key factor contributing to peripheral microvasculopathy and defective angiogenesis in systemic sclerosis. *Ann Rheum Dis* 2016;75:1541-9.
4. Manetti M, Guiducci S, Romano E, *et al.* Decreased expression of the endothelial cell-derived factor EGFL7 in systemic sclerosis: potential contribution to impaired angiogenesis and vasculogenesis. *Arthritis Res Ther* 2013;15:R165.
5. Distler JH, Jüngel A, Huber LC, *et al.* Imatinib mesylate reduces production of extracellular matrix and prevents development of experimental dermal fibrosis. *Arthritis Rheum* 2007;56:311-22.
6. Manetti M, Rosa I, Milia AF, *et al.* Inactivation of urokinase-type plasminogen activator receptor (uPAR) gene induces dermal and pulmonary fibrosis and peripheral microvasculopathy in mice: a new model of experimental scleroderma? *Ann Rheum Dis* 2014;73:1700-9.
7. Manetti M, Rosa I, Fazi M, *et al.* Systemic sclerosis-like histopathological features in the myocardium of uPAR-deficient mice. *Ann Rheum Dis* 2016;75:474-8.
8. Manetti M, Guiducci S, Ruffo M, *et al.* Evidence for progressive reduction and loss of telocytes in the dermal cellular network of systemic sclerosis. *J Cell Mol Med* 2013;17:482-96.

Supplementary table S1. Demographic and clinical characteristics of patients with early diffuse cutaneous systemic sclerosis enrolled for isolation of dermal microvascular endothelial cells and collection of serum samples.

Characteristics	Patients (n = 6)
Mean age, years (range)	37.5 (26-49)
Gender, male/female	1/5
Mean disease duration, months (range)	15.5 (10-22)
Antinuclear antibodies, n	6
Anti-topoisomerase I antibodies, n	4
Mean modified Rodnan skin score (range)	16.2 (10-21)

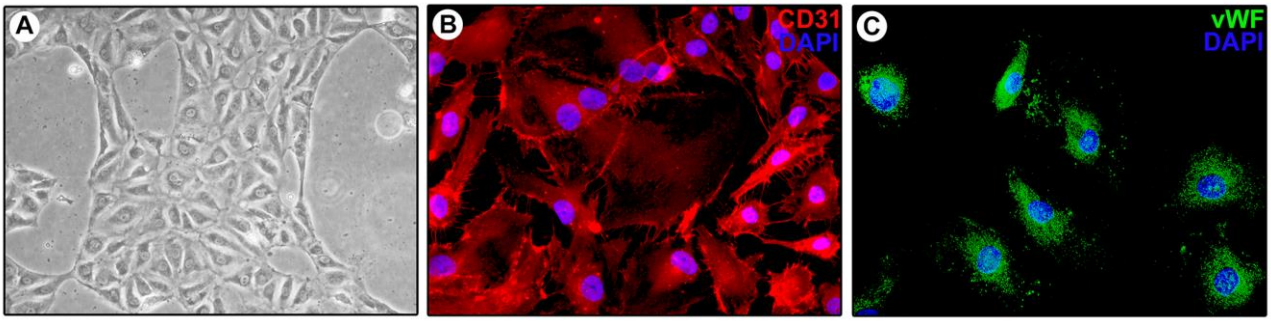

Supplementary figure S1. (A) Representative phase-contrast microphotograph of dermal microvascular endothelial cells (dMVECs) isolated from forearm skin biopsies and subjected to CD31 immunomagnetic isolation by incubation with anti-CD31 conjugated-microbeads. (B and C) Representative fluorescence microphotographs of purified dMVECs immunostained for the endothelial cell markers CD31 (red) (B) and von Willebrand factor (vWF; green) (C). Nuclei are counterstained with 4',6-diamidino-2-phenylindole (DAPI; blue).

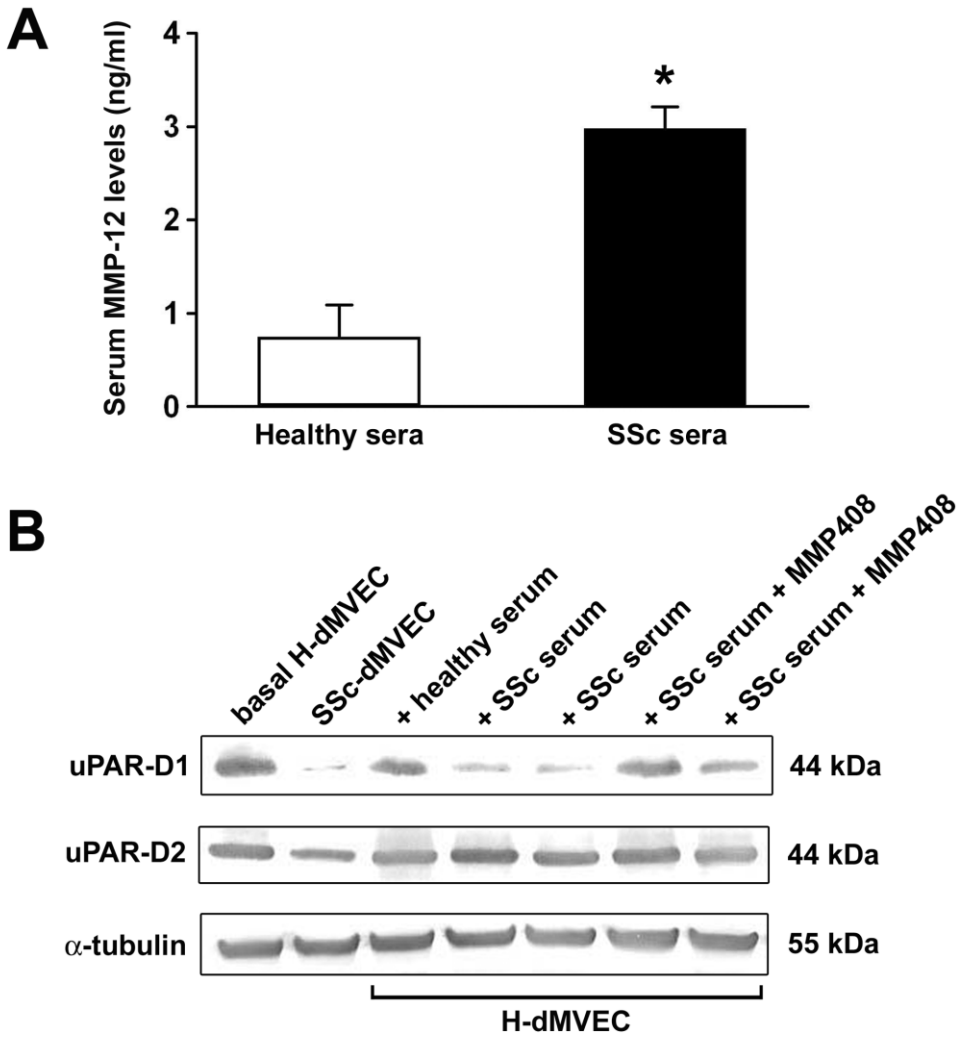

Supplementary figure S2. (A) Levels of matrix metalloproteinase-12 (MMP-12) in serum samples from healthy subjects (n=6) and systemic sclerosis (SSc) patients (n=6) measured by quantitative colorimetric sandwich enzyme-linked immunosorbent assay. Data are mean±SEM. *$p<0.05$ versus healthy sera. (B) Protein levels of urokinase-type plasminogen activator receptor (uPAR) domain 1 (uPAR-D1) and uPAR domain 2 (uPAR-D2) in dermal microvascular endothelial cells (dMVECs) from healthy subjects (H-dMVECs) and SSc patients (SSc-dMVECs) at basal conditions, and in H-dMVECs treated for 24 hours with sera from healthy subjects (n=6), sera from SSc patients (n=6) or SSc sera (n=6) preincubated with the MMP-12 specific inhibitor MMP408. Treatment of H-dMVECs with SSc sera results in uPAR-D1 cleavage similarly to SSc-dMVECs. Healthy sera do not affect uPAR integrity in H-dMVECs. uPAR-D1 cleavage is effectively prevented by preincubation of SSc sera with MMP408. Representative immunoblots are shown. Molecular weight values (kDa) are indicated. Protein expression of α-tubulin was measured as a loading control. Results are representative of three independent experiments performed with three H-dMVEC and three SSc-dMVEC lines.

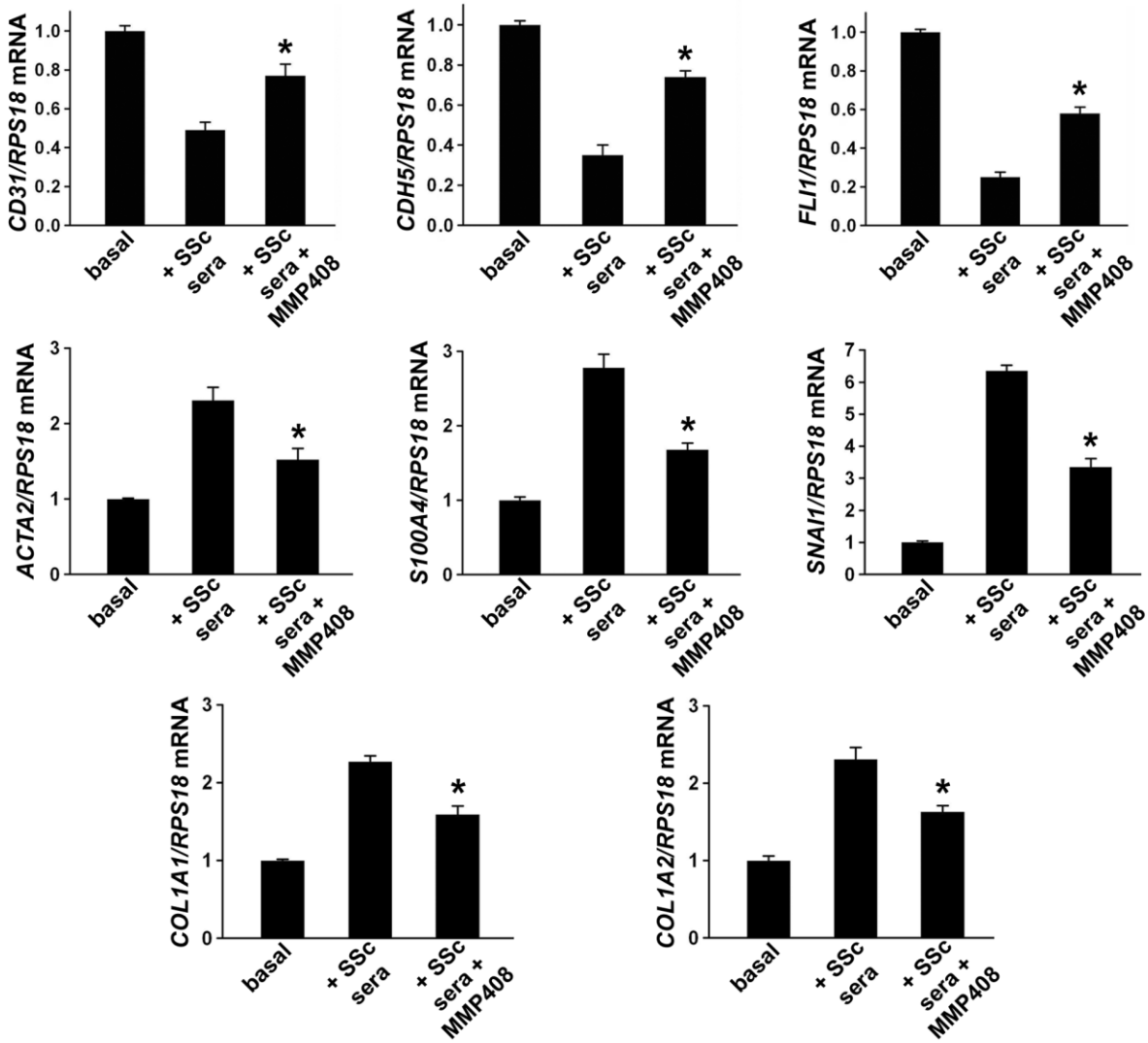

Supplementary figure S3. Preincubation with the matrix metalloproteinase-12 specific inhibitor MMP408 effectively attenuates the effects of sera from patients with systemic sclerosis (SSc) on mRNA expression levels of endothelial and mesenchymal cell markers in healthy dermal microvascular endothelial cells (H-dMVECs). H-dMVECs were treated for 48 hours with sera from SSc patients (n=6), preincubated or not preincubated with MMP408, and subsequently assayed for mRNA expression levels of *CD31*, *CDH5* (VE-cadherin), *FLI1*, *ACTA2* (α-SMA), *S100A4*, *SNAI1* (Snail1), *COL1A1* and *COL1A2* genes by quantitative real-time PCR. Ribosomal protein S18 (*RPS18*) mRNA was measured as an endogenous control for normalisation. The relative values compared with basal H-dMVECs are expressed as mean±SEM of three independent experiments performed with three H-dMVEC lines. *p<0.05 versus H-dMVECs treated with SSc sera not preincubated with MMP408.

Endothelial-to-mesenchymal transition contributes to endothelial dysfunction and dermal fibrosis in systemic sclerosis

Mirko Manetti,[1] Eloisa Romano,[2] Irene Rosa,[1,2] Serena Guiducci,[2] Silvia Bellando-Randone,[2] Amato De Paulis,[3] Lidia Ibba-Manneschi,[1] Marco Matucci-Cerinic[2]

[1]Department of Experimental and Clinical Medicine, Section of Anatomy and Histology, University of Florence, Florence, Italy

[2]Department of Experimental and Clinical Medicine, Section of Internal Medicine, Rheumatology Unit, Azienda Ospedaliero-Universitaria Careggi (AOUC), University of Florence, Florence, Italy

[3]Department of Translational Medical Sciences and Center for Basic and Clinical Immunology Research, University of Naples Federico II, Naples, Italy

Correspondence to

Dr Mirko Manetti,

Department of Experimental and Clinical Medicine,

Section of Anatomy and Histology,

University of Florence,

Largo Brambilla 3,

Florence 50134, Italy;

mirkomanetti@yahoo.it,

mirko.manetti@unifi.it

ABSTRACT

Objective: Systemic sclerosis (SSc) features multiorgan fibrosis orchestrated predominantly by activated myofibroblasts. Endothelial-to-mesenchymal transition (EndoMT) is a transdifferentiation by which endothelial cells (ECs) lose their specific morphology/markers and acquire myofibroblast-like features. Here, we determined the possible contribution of EndoMT to the pathogenesis of dermal fibrosis in SSc and two mouse models.

Methods: Skin sections were immunostained for endothelial CD31 or VE-cadherin in combination with α-smooth muscle actin (α-SMA) myofibroblast marker. Dermal microvascular ECs (dMVECs) were prepared from SSc and healthy skin (SSc-dMVECs and H-dMVECs). H-dMVECs were treated with transforming growth factor-β1 (TGFβ1) or SSc and healthy sera. Endothelial/mesenchymal markers were assessed by real-time PCR, immunoblotting and immunofluorescence. Cell contractile phenotype was assayed by collagen gel contraction.

Results: Cells in intermediate stages of EndoMT were identified in dermal vessels of either SSc patients or bleomycin-induced and urokinase-type plasminogen activator receptor (uPAR)-deficient mouse models. At variance with H-dMVECs, SSc-dMVECs exhibited a spindle-shaped appearance, coexpression of lower levels of CD31 and VE-cadherin with myofibroblast markers (α-SMA+ stress fibres, S100A4 and type I collagen), constitutive nuclear localisation of the EndoMT driver Snail1 and an ability to effectively contract collagen gels. Treatment of H-dMVECs either with SSc sera or TGFβ1 resulted in the acquisition of a myofibroblast-like morphology and contractile phenotype and downregulation of endothelial markers in parallel with the induction of mesenchymal markers. Matrix metalloproteinase-12-dependent uPAR cleavage was implicated in the induction of EndoMT by SSc sera.

Conclusions: In SSc, EndoMT may be a crucial event linking endothelial dysfunction and development of dermal fibrosis.

Keywords: systemic sclerosis, dermal microvascular endothelial cells, myofibroblasts, endothelial-to-mesenchymal transition, dermal fibrosis

INTRODUCTION

Systemic sclerosis (SSc) is a complex connective tissue disease of unknown aetiology characterised by widespread peripheral microvascular injury evolving into progressive fibrosis of skin and multiple internal organs [1-3]. In SSc, fibrosis results from an unrestrained tissue repair process orchestrated predominantly by activated myofibroblasts that are a population of mesenchymal cells displaying unique biological functions. These include an increased synthesis of fibrillar type I and III collagens, a reduction in the expression of genes encoding extracellular matrix (ECM)-degrading enzymes and α-smooth muscle actin (α-SMA) expression and incorporation into stress fibres, which provides an increased contractile force that is crucial for their tissue remodelling properties [4-6]. Indeed, myofibroblast contraction contributes to a large extent to a progressive increase in connective tissue stiffness, a recently recognised potent profibrotic stimulus [7-10].

Given the crucial role of myofibroblasts in the pathogenesis of organ fibrosis in a variety of disorders, considerable attention has been paid to the identification of their putative cellular origins. Hence, extensive investigations have revealed that profibrotic myofibroblasts may arise from different sources including expansion and activation of resident tissue fibroblasts and perivascular pericytes, recruitment of bone marrow-derived circulating precursors, transformation of white adipocytes and transdifferentiation of epithelial cells into mesenchymal cells [4,11-13]. More recently, it has been reported with increasing frequency that vascular endothelial cells (ECs) may also exhibit substantial plasticity by undergoing endothelial-to-mesenchymal transition (EndoMT), a transdifferentiation by which ECs disaggregate, lose polarity and acquire ECM-producing myofibroblast features [14-16]. EndoMT is a phenotypical conversion in which ECs downregulate the expression of their specific markers, such as CD31/platelet-EC adhesion molecule-1, von Willebrand factor (vWF) and vascular endothelial (VE)-cadherin, and acquire mesenchymal cell products including α-SMA, S100A4/fibroblast-specific protein-1 (FSP1) and type I collagen, together with stabilisation and nuclear translocation of the transcriptional regulator Snail1, a crucial trigger of mesenchymal transition [14-16].

To date, EndoMT has emerged as a player in the pathogenesis of tissue fibrosis and fibroproliferative vasculopathy in various diseases, including diabetic nephropathy, cardiac fibrosis, inflammatory bowel disease-related intestinal fibrosis, portal hypertension and primary pulmonary arterial hypertension (PAH) [14,16-21]. Of note, extensive research studies have shown that multiple pathways implicated in SSc pathogenesis, such as transforming growth factor-β (TGFβ), endothelin-1 (ET-1), Notch, Sonic Hedgehog and Wnt pathways, as well as other putative pathways such as oxidative stress and hypoxia, may participate in the molecular mechanisms of the EndoMT

process [16]. For instance, EndoMT can be fully induced by TGFβ in cultured ECs from different tissues [20,22-24].

Although recent studies support the notion that EndoMT may participate in the development of SSc-associated interstitial lung disease (ILD) and PAH [25,26], the occurrence of such a phenotypical change from ECs to activated myofibroblasts has never been demonstrated in the affected skin of SSc patients. Therefore, in the present study we combined ex vivo, in vitro and in vivo approaches to investigate the possible contribution of EndoMT to the pathogenesis of dermal fibrosis in SSc and two mouse models of the disease.

MATERIALS AND METHODS

An extended methods section is provided in the online supplementary material.

Cell culture and reagents

Primary cultures of dermal microvascular ECs (dMVECs) were established by explantation from biopsies of the lesional forearm skin from 6 patients with early diffuse cutaneous SSc (dcSSc; disease duration <2 years from first non-Raynaud symptom) [27] and from 6 healthy adult subjects under protocols approved by the local institutional review board at the Azienda Ospedaliero-Universitaria Careggi (AOUC), Florence, Italy. Skin biopsies were processed as previously described [28,29]. Patient characteristics are summarised in online supplementary table S1. Adherent cells were detached and subjected to CD31 immunomagnetic isolation by incubation with anti-CD31 conjugated-microbeads [28,29]. Isolated cells were further identified as ECs by labelling with anti-factor VIII-related antigen (vWF) and anti-CD105, followed by reprobing with anti-CD31 antibodies (see online supplementary figure S1). dMVECs from healthy subjects (H-dMVECs) and SSc patients (SSc-dMVECs) were maintained as detailed in the online supplementary material. In selected experiments, H-dMVECs were treated with recombinant human TGFβ1 (10 ng/ml; PeproTech, Rocky Hill, NJ, USA) or 10% serum from early dcSSc patients (n=6) and healthy subjects (n=6) for 24, 48 and 72 hours. In some experimental points, sera were preincubated with the matrix metalloproteinase-12 (MMP-12) specific inhibitor MMP408 (10 nM; Sigma-Aldrich, St. Louis, MO, USA) before cell stimulation.

Fluorescence immunocytochemistry

At the end of the experiments, cells were fixed with 3.7% buffered paraformaldehyde and immunofluorescence with antibodies against CD31, VE-cadherin, α-SMA, S100A4/FSP1, type I

collagen and Snail1 (all from Abcam, Cambridge, UK) was performed as detailed in the online supplementary material. In some specimens, Alexa 488-labelled phalloidin (Invitrogen, Carlsbad, CA, USA) was applied to the cells to visualise the arrangement of the F-actin cytoskeleton. For primary and secondary antibodies, refer to the online supplementary material.

RNA isolation and quantitative real-time PCR

At the end of the experiments, cultures were harvested and total RNA was isolated using the RNeasy Micro Kit (Qiagen, Milan, Italy). First strand cDNA synthesis and mRNA quantification by SYBR Green real-time PCR were performed as reported elsewhere [29]. For predesigned oligonucleotide primer pairs, refer to the online supplementary material.

Immunoblotting

Whole cell protein lysates from dMVECs were subjected to immunoblot analysis as described elsewhere [29]. For details on primary antibodies against CD31, VE-cadherin, α-SMA, S100A4/FSP1, type I collagen, Snail1, Friend leukemia integration-1 (Fli1), urokinase-type plasminogen activator receptor (uPAR) domain 1 (D1) and domain 2 and α-tubulin, refer to the online supplementary material.

Collagen gel contraction assay

Collagen gel contraction assays were performed as described in the online supplementary material.

Enzyme-linked immunosorbent assay

Levels of MMP-12 in serum samples were measured by quantitative enzyme-linked immunosorbent assay as described in the online supplementary material.

Fluorescence immunohistochemistry on human and mouse skin

Paraffin-embedded sections of lesional forearm skin biopsies were obtained from 12 SSc patients (n=4 with limited cutaneous SSc and n=8 with dcSSc) and 10 age-matched and gender-matched healthy donors, as described elsewhere [28-30]. Skin sections from two mouse models of dermal fibrosis were also used. First, 6 week-old male C57BL/6 mice (Charles River Laboratories, Calco, Lecco, Italy) received subcutaneous injections of 100 µl of bleomycin dissolved in 0.9% NaCl (saline solution) at a concentration of 0.5 mg/ml every other day for 4 weeks in well-defined areas of the upper back. Subcutaneous injections of 0.9% NaCl served as controls [31]. The second model consisted of 12 week-old male uPAR-deficient mice and wild-type littermates as described

elsewhere [32,33]. All animal protocols were performed in accordance with DL 116/92 and approved by the Institutional Animal Care and Use Committee of the University of Florence. Each experimental group consisted of at least six mice. Double-label immunofluorescence using antibodies against α-SMA and CD31 or VE-cadherin was carried out as detailed in the online supplementary material. The percentage of dermal vessels displaying CD31/α-SMA and VE-cadherin/α-SMA colocalisation was determined in five randomly selected high-power fields of the dermis from each of three sections per sample.

Transmission electron microscopy

Ultrathin skin sections from 5 dcSSc patients and 5 healthy controls were processed and examined according to previously published protocols [34] as detailed in the online supplementary material.

Statistical analysis

Statistical analyses were performed using the Statistical Package for Social Sciences software for Windows, V.20.0 (SPSS, Chicago, IL, USA). Data are expressed as means and standard errors of the mean (SEM). The Student's t-test was used for statistical evaluation of the differences between two independent groups. A p value of <0.05 according to a two-tailed distribution was considered statistically significant.

RESULTS

EndoMT in dermal vessels of SSc patients and experimental models of SSc

In order to determine ex vivo the presence of transitional EndoMT cells, skin sections from SSc patients and healthy donors were subjected to double immunofluorescence staining for the EC markers CD31 or VE-cadherin and the myofibroblast marker α-SMA. In the healthy dermal microvasculature, α-SMA expression was mostly restricted to pericytes and vascular smooth muscle cells surrounding the endothelial layer (figure 1A). On the contrary, we observed colocalised CD31/α-SMA and VE-cadherin/α-SMA in the endothelium of numerous dermal capillary vessels and arterioles from SSc patients, suggestive for cells in intermediate stages of EndoMT (figure 1A). Indeed, the percentage of vessels displaying CD31/α-SMA and VE-cadherin/α-SMA colocalisation was significantly increased in skin biopsies from SSc patients compared with healthy skin ($p<0.001$ for both) (figure 1B). No difference in the frequency of transitional EndoMT cells was observed between SSc cutaneous subsets (data not shown). Furthermore, transmission electron microscopy

analysis revealed that the presence of vWF-storing Weibel-Palade bodies was clearly reduced in SSc dermal endothelium (figure 1C).

Next we investigated in vivo the presence of transitional EndoMT cells in the skin of two mouse models of SSc, namely mice with bleomycin-induced dermal fibrosis and uPAR-deficient mice [31-33]. The frequency of transitional EndoMT cells in murine skin was assessed by colocalisation of either CD31 or VE-cadherin and α-SMA. As displayed in figure 2, using both marker combinations we observed transitional EndoMT cells to be present at very low levels in saline-treated control mice, with significantly higher levels in the bleomycin treatment group ($p<0.001$ for both). Similarly, a significantly higher percentage of vessels with CD31/α-SMA and VE-cadherin/α-SMA double-positive cells was detected in the dermis of uPAR-deficient mice compared with wild-type littermates ($p<0.001$ for both) (figure 2A,B).

Cultured SSc-dMVECs coexpress endothelial and mesenchymal cell markers and exhibit a myofibroblast-like functional phenotype

The expression of endothelial and mesenchymal cell markers in dMVECs isolated from forearm skin biopsies was investigated by immunofluorescence and immunoblotting. In agreement with previous reports [28,35], H-dMVECs exhibited a typical endothelial morphology with a polygonal shape, whereas the majority of SSc-dMVECs had an elongated shape often characterised by branches (figure 3A). Both H-dMVECs and SSc-dMVECs were immunopositive for the pan-EC marker CD31 (figure 3A). However, the expression of CD31 and VE-cadherin was markedly decreased in SSc-dMVECs compared with H-dMVECs (figure 3A). SSc-dMVECs also expressed α-SMA, which often was incorporated into stress fibres, as well as S100A4/FSP1 and type I collagen (figure 3A). On the contrary, as expected, in H-dMVECs there was no evidence of α-SMA and type I collagen expression, and S100A4/FSP1 was almost undetectable (figure 3A). Double immunofluorescence staining clearly revealed the unique presence of numerous CD31+ cells displaying α-SMA+ stress fibres in SSc-dMVEC cultures compared with H-dMVECs ($p<0.001$) (figure 3B). Phalloidin staining further revealed that while H-dMVECs showed a weak and disorganised expression of F-actin fibres, SSc-dMVECs exhibited a marked increase in stress fibres mainly organised longitudinally (figure 3A). Furthermore, we investigated the expression of Snail1, a zinc-finger transcription factor that induces numerous transcriptional events leading to the acquisition of a mesenchymal cell-specific phenotype such as stimulation of α-SMA expression [16,24]. As displayed in figure 3A, strong expression and nuclear localisation of Snail1 were constitutively detected in SSc-dMVECs, while Snail1 expression was negligible in H-dMVECs. Immunoblot analyses confirmed either a significantly lower protein expression of CD31 and VE-

cadherin or a significantly higher expression of α-SMA, S100A4/FSP1, type I collagen and Snail1 in SSc-dMVECs compared with H-dMVECs ($p<0.001$ for all comparisons) (figure 3C). According to the immunofluorescence data, both α-SMA and type I collagen were undetectable in protein lysates from H-dMVECs (figure 3C). Moreover, SSc-dMVECs exhibited a significant reduction in protein expression of Fli1 ($p<0.001$ versus H-dMVECs) (figure 3C), a transcription factor which plays a pivotal role in the maintenance of EC homeostasis and whose deficiency may be implicated in EndoMT [36-38]. The occurrence of EndoMT was confirmed functionally by the evidence that SSc-dMVECs were able to effectively contract collagen gels (figure 3D).

Treatment with SSc sera induces a myofibroblast-like phenotype in H-dMVECs

Previous studies have demonstrated that treatment with sera from SSc patients impairs the angiogenic performance of H-dMVECs in vitro [29,39,40]. Nevertheless, whether these antiangiogenic effects may be in part related to the induction of the EndoMT process has never been investigated. To address this issue, H-dMVECs were challenged with sera from early dcSSc patients and healthy subjects and subsequently assayed for changes in cell morphology and the expression of endothelial and mesenchymal cell markers. According to the literature [20,22-24], stimulation with recombinant human TGFβ1 was performed in parallel as a positive control of EndoMT. After 48-hour treatment with SSc sera, H-dMVECs started to disaggregate losing their characteristic polygonal cobblestone-like morphology (figure 4A). These changes progressed rapidly with the appearance of numerous cells exhibiting a spindle-shaped morphology in H-dMVEC cultures treated with SSc sera for 72 hours (figure 4A). As expected, similar findings were observed when H-dMVECs were challenged with TGFβ1, whereas H-dMVEC morphology did not change over time in cultures treated with healthy sera (figure 4A). Indeed, 72-hour treatment either with SSc sera or TGFβ1 induced a significant increase in the percentage of spindle-shaped cells (both $p<0.001$ versus basal H-dMVECs) (figure 4A) which were able to effectively contract collagen gels (figure 4B).

As displayed in figure 5, real-time PCR analysis revealed a significant reduction in mRNA levels of *CD31*, *CDH5* and *FLI1* genes in H-dMVECs treated either with SSc sera or TGFβ1 for 48 hours (all $p<0.001$ versus basal H-dMVECs). This happened in parallel with the induction of *ACTA2*, *S100A4*, *SNAI1*, *COL1A1* and *COL1A2* mRNA expression (all $p<0.001$ versus basal H-dMVECs) (figure 5). On the contrary, 48-hour treatment of H-dMVECs with healthy sera did not affect mRNA expression levels of the aforementioned markers (figure 5). These results were confirmed by immunoblot and immunofluorescence assessment of endothelial and mesenchymal protein expression levels in cells treated for 72 hours (figure 6A-G). In particular, both untreated cells and

those treated with healthy sera showed no expression of α-SMA and type I collagen along with very low levels of Snail1, whereas treatment either with SSc sera or TGFβ1 induced the appearance of α-SMA+ stress fibres, de novo synthesis of type I collagen and strong expression and nuclear localisation of Snail1 (figure 6B-G).

MMP-12-dependent cleavage of uPAR is implicated in the induction of EndoMT by SSc sera

We previously demonstrated that in SSc-dMVECs, uPAR undergoes a MMP-12-dependent cleavage of domain D1 resulting in impaired angiogenesis [35,41]. Interestingly, the cleavage of uPAR-D1 was shown to be a crucial step in fibroblast-to-myofibroblast transition [42]. Therefore, we herein investigated whether MMP-12-dependent uPAR-D1 cleavage could be implicated in the induction of EndoMT by SSc sera. Consistent with previous reports [40,43], MMP-12 levels were raised in SSc sera (see online supplementary figure S2A). Treatment of H-dMVECs with SSc sera resulted in uPAR-D1 cleavage already after 24 hours (see online supplementary figure S2B). Such a cleavage was instead prevented when SSc sera were preincubated with the MMP-12 specific inhibitor MMP408 (see online supplementary figure S2B). As shown in online supplementary figure S3, preincubation with MMP408 significantly blunted the effects of 48-hour treatment with SSc sera on gene expression of endothelial and mesenchymal cell markers.

DISCUSSION

Our data provide the first direct evidence that EndoMT may take place in the skin of SSc patients and may have therefore a role in the pathogenesis of dermal fibrosis. The ex vivo immunohistological data clearly demonstrate the presence of transitional EndoMT cells simultaneously expressing EC and myofibroblast markers in SSc dermal microvasculature. In contrast, EndoMT was only observed at negligible levels in control skin. These results are substantially in agreement with similar findings recently described in the pulmonary vessels of patients with SSc-associated ILD and PAH [25,26]. We have further characterised in vitro the phenotype of dMVECs isolated from SSc skin and found that these cells are in an intermediate state between an EC and a myofibroblast-like contractile phenotype, combining markers of both cell types. The results also show that H-dMVECs can undergo EndoMT in response to treatment with SSc sera, thus supporting the hypothesis that such cellular transdifferentiation may be operative in SSc. In fact, after a prolonged challenge with SSc sera, H-dMVECs lost their typical endothelial cobblestone appearance and acquired myofibroblast-like structural and functional features. Consistent with these morphofunctional changes, SSc serum-treated H-dMVECs exhibited a reduction in the expression of EC markers CD31 and VE-cadherin and an upregulation of

mesenchymal markers, including α-SMA+ stress fibres, S100A4/FSP1, type I collagen and nuclear Snail1. Furthermore, the presence of transitional EndoMT cells in dermal vessels of two murine models of SSc is a matter of interest. Indeed, previous studies have demonstrated the occurrence of EndoMT in animal models of cardiac, pulmonary and renal fibrosis, as well as in models of PAH [16,23,26,44,45]. Although our experimental data support the notion that EndoMT may contribute to the accumulation of myofibroblasts and the development of dermal fibrosis in vivo, this needs to be further confirmed by using lineage tracing in different preclinical models of SSc.

Besides the increase in the number of profibrotic myofibroblasts, EndoMT may favour microvascular derangement and loss of ECs contributing to capillary rarefaction, impaired angiogenesis and chronic tissue ischaemia in SSc skin. Indeed, endothelial dysfunction is considered a pivotal factor contributing to peripheral vessel remodelling in SSc [3,15,41]. A defective response to proangiogenic stimuli and several functional defects, such as an impaired ability to organise into capillary-like tubes in vitro, have been extensively reported in SSc-dMVECs [28,29,35,41,46]. Moreover, transcriptome profiling studies have revealed profound differences in the expression of genes encoding a variety of angiogenic regulators between SSc-dMVECs and H-dMVECs [41,47]. In this context, our present findings shed light on EndoMT as a pathogenic mechanism that in SSc may directly link EC dysfunction to the development of dermal fibrosis. The intrinsic propensity of SSc-dMVECs to transition towards a profibrotic myofibroblast-like phenotype might in effect largely explain their well-known defective angiogenic behaviour. In addition, here we clearly demonstrate that a prolonged treatment with sera from SSc patients is capable of sustaining the EndoMT process in H-dMVECs. Of note, shorter time treatments with SSc sera have previously been shown to impair angiogenesis and survival of H-dMVECs [29,39,40]. Mechanistically, our present findings show that MMP-12-dependent cleavage of uPAR, a process which has been deeply implicated either in the impaired angiogenic performance of SSc-dMVECs or in fibroblast-to-myofibroblast differentiation [35,41,42], takes part in the pro-EndoMT effect exerted by SSc sera. Besides MMP-12, additional as yet unidentified circulating factors might trigger EndoMT and the loss of microvascular integrity in SSc dermis. Though further in-depth studies will be required, potential candidates include a large array of mediators which are elevated in SSc and have been demonstrated to induce EndoMT in vitro, such as TGFβ1, ET-1, tumour necrosis factor-α, asymmetric dimethylarginine and endostatin [16,19,26,48,49]. Consistent with our in vitro observations, a recent study reported that sera from patients with chronic kidney disease induced EndoMT, decreased proliferation and increased apoptosis of human coronary artery ECs [49]. These effects were mainly attributable to increased concentrations of circulating angiogenesis and nitric oxide inhibitors [49]. Finally, when considering the autoimmune background of SSc, we

cannot exclude the possible implication of functional (agonistic) autoantibodies against cell surface receptors in the EndoMT process. Indeed, a high proportion of SSc patients display agonistic autoantibodies against the angiotensin II type 1 receptor and the ET-1 type A receptor which can induce a variety of cellular responses such as production of TGFβ by dMVECs and synthesis of type I collagen by skin fibroblasts [50]. Further mechanistic studies aimed at identifying key initiators of EndoMT in SSc are warranted.

In summary, our data collectively support the notion that EndoMT is a process occurring in the dermal endothelium of SSc patients, where it may represent a crucial link between EC dysfunction and development of fibrosis. Hence, preventing or blocking EndoMT might be a novel and useful approach to treat peripheral microvasculopathy and prevent, at least in part, skin fibrosis in SSc patients.

Contributors

Study conception and design: MM, ER, LI-M and MM-C. Acquisition of data: MM, ER, IR, SG, SB-R, ADP, LI-M and MM-C. Interpretation of data: MM, ER, IR, LI-M and MM-C. Manuscript preparation: MM and MM-C.

Funding

Supported by grants from the University of Florence (Progetti di Ricerca di Ateneo to LI-M and MM-C).

Competing interests

None declared.

Ethics approval

The study was approved by the local institutional review board at the Azienda Ospedaliero-Universitaria Careggi (AOUC), Florence, Italy, and all subjects provided written informed consent.

REFERENCES

1. Allanore Y, Simms R, Distler O, *et al.* Systemic sclerosis. *Nat Rev Dis Primers* 2015;1:15002.
2. Gabrielli A, Avvedimento EV, Krieg T. Scleroderma. *N Engl J Med* 2009;360:1989-2003.
3. Matucci-Cerinic M, Kahaleh B, Wigley FM. Evidence that systemic sclerosis is a vascular disease. *Arthritis Rheum* 2013;65:1953-62.
4. Hinz B, Phan SH, Thannickal VJ, *et al.* Recent developments in myofibroblast biology: paradigms for connective tissue remodeling. *Am J Pathol* 2012;180:1340-55.
5. Hu B, Phan SH. Myofibroblasts. *Curr Opin Rheumatol* 2013;25:71-7.
6. Kis K, Liu X, Hagood JS. Myofibroblast differentiation and survival in fibrotic disease. *Expert Rev Mol Med* 2011;13:e27.
7. Hinz B. The extracellular matrix and transforming growth factor-β1: Tale of a strained relationship. *Matrix Biol* 2015;47:54-65.
8. Hinz B. The myofibroblast: paradigm for a mechanically active cell. *J Biomech* 2010;43:146-55.
9. Huang X, Yang N, Fiore VF, *et al.* Matrix stiffness-induced myofibroblast differentiation is mediated by intrinsic mechanotransduction. *Am J Respir Cell Mol Biol* 2012;47:340-8.
10. Gerber EE, Gallo EM, Fontana SC, *et al.* Integrin-modulating therapy prevents fibrosis and autoimmunity in mouse models of scleroderma. *Nature* 2013;503:126-30.
11. Hinz B, Phan SH, Thannickal VJ, *et al.* The myofibroblast: one function, multiple origins. *Am J Pathol* 2007;170:1807-16.
12. Ebmeier S, Horsley V. Origin of fibrosing cells in systemic sclerosis. *Curr Opin Rheumatol* 2015;27:555-62.
13. Marangoni RG, Korman BD, Wei J, *et al.* Myofibroblasts in murine cutaneous fibrosis originate from adiponectin-positive intradermal progenitors. *Arthritis Rheumatol* 2015;67:1062-73.
14. Piera-Velazquez S, Li Z, Jimenez SA. Role of endothelial-mesenchymal transition (EndoMT) in the pathogenesis of fibrotic disorders. *Am J Pathol* 2011;179:1074-80.
15. Manetti M, Guiducci S, Matucci-Cerinic M. The origin of the myofibroblast in fibroproliferative vasculopathy: does the endothelial cell steer the pathophysiology of systemic sclerosis? *Arthritis Rheum* 2011;63:2164-7.
16. Jimenez SA, Piera-Velazquez S. Endothelial to mesenchymal transition (EndoMT) in the pathogenesis of Systemic Sclerosis-associated pulmonary fibrosis and pulmonary arterial hypertension. Myth or reality? *Matrix Biol* 2016;51:26-36.

17. He J, Xu Y, Koya D, *et al.* Role of the endothelial-to-mesenchymal transition in renal fibrosis of chronic kidney disease. *Clin Exp Nephrol* 2013;17:488-97.
18. Li J, Bertram JF. Review: Endothelial-myofibroblast transition, a new player in diabetic renal fibrosis. *Nephrology (Carlton)* 2010;15:507-12.
19. Rieder F, Kessler SP, West GA, *et al.* Inflammation-induced endothelial-to-mesenchymal transition: a novel mechanism of intestinal fibrosis. *Am J Pathol* 2011;179:2660-73.
20. Kitao A, Sato Y, Sawada-Kitamura S, *et al.* Endothelial to mesenchymal transition via transforming growth factor-beta1/Smad activation is associated with portal venous stenosis in idiopathic portal hypertension. *Am J Pathol* 2009;175:616-26.
21. Ranchoux B, Antigny F, Rucker-Martin C, *et al.* Endothelial-to-mesenchymal transition in pulmonary hypertension. *Circulation* 2015;131:1006-18.
22. Arciniegas E, Sutton AB, Allen TD, *et al.* Transforming growth factor beta 1 promotes the differentiation of endothelial cells into smooth muscle-like cells in vitro. *J Cell Sci* 1992;103:521-9.
23. Zeisberg EM, Potenta SE, Sugimoto H, *et al.* Fibroblasts in kidney fibrosis emerge via endothelial-to-mesenchymal transition. *J Am Soc Nephrol* 2008;19:2282-7.
24. Li Z, Jimenez SA. Protein kinase Cδ and c-Abl kinase are required for transforming growth factor β induction of endothelial-mesenchymal transition in vitro. *Arthritis Rheum* 2011;63:2473-83.
25. Mendoza FA, Piera-Velazquez S, Farber JL, *et al.* Endothelial cells expressing endothelial and mesenchymal cell gene products in lung tissue from patients with systemic sclerosis-associated interstitial lung disease. *Arthritis Rheumatol* 2016;68:210-7.
26. Good RB, Gilbane AJ, Trinder SL, *et al.* Endothelial to mesenchymal transition contributes to endothelial dysfunction in pulmonary arterial hypertension. *Am J Pathol* 2015;185:1850-8.
27. van den Hoogen F, Khanna D, Fransen J, *et al.* 2013 classification criteria for systemic sclerosis: an American college of rheumatology/European league against rheumatism collaborative initiative. *Ann Rheum Dis* 2013;72:1747-55.
28. Manetti M, Guiducci S, Romano E, *et al.* Overexpression of VEGF165b, an inhibitory splice variant of vascular endothelial growth factor, leads to insufficient angiogenesis in patients with systemic sclerosis. *Circ Res* 2011;109:e14-26.
29. Romano E, Chora I, Manetti M, *et al.* Decreased expression of neuropilin-1 as a novel key factor contributing to peripheral microvasculopathy and defective angiogenesis in systemic sclerosis. *Ann Rheum Dis* 2016;75:1541-9.

30. Manetti M, Guiducci S, Romano E, *et al.* Decreased expression of the endothelial cell-derived factor EGFL7 in systemic sclerosis: potential contribution to impaired angiogenesis and vasculogenesis. *Arthritis Res Ther* 2013;15:R165.
31. Distler JH, Jüngel A, Huber LC, *et al.* Imatinib mesylate reduces production of extracellular matrix and prevents development of experimental dermal fibrosis. *Arthritis Rheum* 2007;56:311-22.
32. Manetti M, Rosa I, Milia AF, *et al.* Inactivation of urokinase-type plasminogen activator receptor (uPAR) gene induces dermal and pulmonary fibrosis and peripheral microvasculopathy in mice: a new model of experimental scleroderma? *Ann Rheum Dis* 2014;73:1700-9.
33. Manetti M, Rosa I, Fazi M, *et al.* Systemic sclerosis-like histopathological features in the myocardium of uPAR-deficient mice. *Ann Rheum Dis* 2016;75:474-8.
34. Manetti M, Guiducci S, Ruffo M, *et al.* Evidence for progressive reduction and loss of telocytes in the dermal cellular network of systemic sclerosis. *J Cell Mol Med* 2013;17:482-96.
35. Margheri F, Manetti M, Serrati S, *et al.* Domain 1 of the urokinase-type plasminogen activator receptor is required for its morphologic and functional, beta2 integrin-mediated connection with actin cytoskeleton in human microvascular endothelial cells: failure of association in systemic sclerosis endothelial cells. *Arthritis Rheum* 2006;54:3926-38.
36. Asano Y, Stawski L, Hant F, *et al.* Endothelial Fli1 deficiency impairs vascular homeostasis: a role in scleroderma vasculopathy. *Am J Pathol* 2010;176:1983-98.
37. Taniguchi T, Asano Y, Akamata K, *et al.* Fibrosis, vascular activation, and immune abnormalities resembling systemic sclerosis in bleomycin-treated Fli-1-haploinsufficient mice. *Arthritis Rheumatol* 2015;67:517-26.
38. Manetti M. Fli1 deficiency and beyond: a unique pathway linking peripheral vasculopathy and dermal fibrosis in systemic sclerosis. *Exp Dermatol* 2015;24:256-7.
39. Romano E, Bellando-Randone S, Manetti M, *et al.* Bosentan blocks the antiangiogenic effects of sera from systemic sclerosis patients: an in vitro study. *Clin Exp Rheumatol* 2015;33(4 Suppl 91):S148-52.
40. Borghini A, Manetti M, Nacci F, *et al.* Systemic sclerosis sera impair angiogenic performance of dermal microvascular endothelial cells: therapeutic implications of cyclophosphamide. *PLoS One* 2015;10:e0130166.
41. Manetti M, Guiducci S, Ibba-Manneschi L, *et al.* Mechanisms in the loss of capillaries in systemic sclerosis: angiogenesis versus vasculogenesis. *J Cell Mol Med* 2010;14:1241-54.

42. Bernstein AM, Twining SS, Warejcka DJ, *et al.* Urokinase receptor cleavage: a crucial step in fibroblast-to-myofibroblast differentiation. *Mol Biol Cell* 2007;18:2716-27.
43. Manetti M, Guiducci S, Romano E, *et al.* Increased serum levels and tissue expression of matrix metalloproteinase-12 in patients with systemic sclerosis: correlation with severity of skin and pulmonary fibrosis and vascular damage. *Ann Rheum Dis* 2012;71:1064-72.
44. Hashimoto N, Phan SH, Imaizumi K, *et al.* Endothelial-mesenchymal transition in bleomycin-induced pulmonary fibrosis. *Am J Respir Cell Mol Biol* 2010;43:161-72.
45. Zeisberg EM, Tarnavski O, Zeisberg M, *et al.* Endothelial-to-mesenchymal transition contributes to cardiac fibrosis. *Nat Med* 2007;13:952-61.
46. Tsou PS, Rabquer BJ, Ohara RA, *et al.* Scleroderma dermal microvascular endothelial cells exhibit defective response to pro-angiogenic chemokines. *Rheumatology (Oxford)* 2016;55:745-54.
47. Giusti B, Fibbi G, Margheri F, *et al.* A model of anti-angiogenesis: differential transcriptosome profiling of microvascular endothelial cells from diffuse systemic sclerosis patients. *Arthritis Res Ther* 2006;8:R115.
48. Wermuth PJ, Li Z, Mendoza FA, *et al.* Stimulation of transforming growth factor-β1-induced endothelial-to-mesenchymal transition and tissue fibrosis by endothelin-1 (ET-1): a novel profibrotic effect of ET-1. *PLoS One* 2016;11:e0161988.
49. Charytan DM, Padera R, Helfand AM, *et al.* Increased concentration of circulating angiogenesis and nitric oxide inhibitors induces endothelial to mesenchymal transition and myocardial fibrosis in patients with chronic kidney disease. *Int J Cardiol* 2014;176:99-109.
50. Cabral-Marques O, Riemekasten G. Vascular hypothesis revisited: Role of stimulating antibodies against angiotensin and endothelin receptors in the pathogenesis of systemic sclerosis. *Autoimmun Rev* 2016;15:690-4.

FIGURE LEGENDS

Figure 1. Detection of endothelial-to-mesenchymal transition (EndoMT) in dermal vessels of patients with systemic sclerosis (SSc). (A) Representative fluorescence microphotographs of skin sections from healthy controls and patients with SSc double immunostained for the endothelial cell (EC) markers CD31 or VE-cadherin (red) and the myofibroblast marker α-smooth muscle actin (α-SMA; green) and counterstained with 4',6-diamidino-2-phenylindole (DAPI; blue) for nuclei. In healthy dermal vessels, α-SMA expression is mostly restricted to pericytes and vascular smooth muscle cells surrounding ECs. In SSc skin, colocalised CD31/α-SMA and VE-cadherin/α-SMA give rise to yellow staining which is evident in transitional EndoMT cells of numerous capillary vessels (arrows) and arterioles (arrowheads). In each panel, insets show higher magnification views of dermal microvessels. Scale bar=50 μm. (B) The percentage of dermal vessels displaying CD31/α-SMA and VE-cadherin/α-SMA colocalisation is significantly increased in skin biopsies from SSc patients (n=12) compared with healthy skin (n=10). Data are mean±SEM. *$p<0.001$ versus healthy skin. (C) Representative transmission electron microscopy microphotographs of dermal capillary vessels from healthy controls (n=5) and patients with SSc (n=5). At least eight capillary vessels from each of three ultrathin sections per sample were analysed. Numerous Weibel-Palade bodies (arrows) are present in healthy dermal ECs, while they are reduced or even absent in SSc dermal ECs. Scale bar=2 μm.

Figure 2. Detection of endothelial-to-mesenchymal transition (EndoMT) in dermal vessels of murine models of systemic sclerosis (SSc). (A and B) Representative fluorescence microphotographs of mouse skin sections double immunostained for either CD31 (red) (A) or VE-cadherin (red) (B) endothelial cell markers and the myofibroblast marker α-smooth muscle actin (α-SMA; green) with 4',6-diamidino-2-phenylindole (DAPI; blue) counterstain for nuclei are shown. In the dermis of bleomycin-treated mice and urokinase-type plasminogen activator receptor (uPAR)-deficient mice, colocalisation of either CD31 or VE-cadherin and α-SMA gives rise to yellow staining which is evident in transitional EndoMT cells of numerous microvessels (arrows). Insets show higher magnification views of dermal microvessels from the corresponding panels. Scale bar=50 μm. The percentage of dermal vessels displaying CD31/α-SMA or VE-cadherin/α-SMA colocalisation is reported in the histograms. Data are mean±SEM (6 mice in each experimental group). *$p<0.001$ versus saline-treated mice (A and B, top), *$p<0.001$ versus wild-type littermates (A and B, bottom).

Figure 3. Dermal microvascular endothelial cells (dMVECs) isolated from systemic sclerosis (SSc) skin coexpress endothelial and mesenchymal cell markers and exhibit a myofibroblast-like functional phenotype. (A) Representative fluorescence microphotographs of healthy dMVECs (H-dMVECs) and SSc-dMVECs (n=6 each) immunostained for CD31, VE-cadherin, α-smooth muscle actin (α-SMA), F-actin (phalloidin), S100A4/fibroblast-specific protein-1 (FSP1), type I collagen and Snail1 transcription factor. Nuclei are counterstained with 4',6-diamidino-2-phenylindole (DAPI). Both H-dMVECs and SSc-dMVECs are immunopositive for the pan-endothelial cell marker CD31. The expression of CD31 and VE-cadherin is markedly lower in SSc-dMVECs compared with H-dMVECs. SSc-dMVECs exhibit α-SMA+ stress fibres (shown at higher magnification in the inset), a marked increase in phalloidin+ stress fibres mainly organised longitudinally, and expression of S100A4/FSP1, type I collagen and nuclear Snail1. In H-dMVECs, α-SMA and type I collagen are undetectable, while expression of S100A4/FSP1 and Snail1 is negligible. Scale bar=50 μm. (B) Representative fluorescence microphotographs of SSc-dMVECs double immunostained for CD31 (red) and α-SMA (green) with DAPI (blue) counterstain for nuclei. Note the presence of CD31+ cells displaying α-SMA+ stress fibres. Cells labelled as (1) and (2) in the left panel are shown at higher magnification in the right panels. The degree of α-SMA arrangement into stress fibres varies among cells. Scale bar=50 μm (left panel), 20 μm (right

panels). The percentage of CD31/α-SMA double-positive cells is reported in the histograms. Data are mean±SEM. *p<0.001 versus H-dMVECs. (C) Protein lysates from H-dMVECs and SSc-dMVECs were assayed for the expression of CD31, VE-cadherin, α-SMA, S100A4/FSP1, type I collagen, Snail1 and Friend leukemia integration-1 (Fli1). Representative immunoblots are shown. Molecular weight values (kDa) are indicated. The densitometric analysis of the bands normalised to α-tubulin is reported in the histograms. Data are mean±SEM of optical density in arbitrary units (a.u.). *p<0.001 versus H-dMVECs. Results are representative of three independent experiments performed with each of the six H-dMVEC and SSc-dMVEC lines. (D) Collagen gel contraction assay with H-dMVECs and SSc-dMVECs (n=6 each). Gel size in the presence of SSc-dMVECs is expressed as percentage of that observed in the presence of H-dMVECs. Data are mean±SEM. *p<0.001 versus H-dMVECs.

Figure 4. Treatment with sera from patients with systemic sclerosis (SSc) induces a myofibroblast-like morphology and functional phenotype in healthy dermal microvascular endothelial cells (H-dMVECs). (A) Representative phase-contrast microphotographs of H-dMVECs (n=3) at baseline and after treatment for 48 and 72 hours (h) with sera from healthy subjects (n=6), sera from patients with SSc (n=6) or recombinant human transforming growth factor-β1 (rh TGFβ1; 10 ng/ml) are shown (x10 original magnification). The morphology of H-dMVECs does not change over time in cultures treated with healthy sera. After 48-hour treatment either with SSc sera or rh TGFβ1, H-dMVECs start to disaggregate and lose their characteristic polygonal cobblestone-like morphology. Cells exhibiting a spindle-shaped morphology are clearly veasible in H-dMVEC cultures treated either with SSc sera or rh TGFβ1 for 72 hours. The percentage of spindle-shaped cells is reported in the histograms. Data are mean±SEM. *p<0.001 versus basal H-dMVECs. (B) Collagen gel contraction assay with H-dMVECs at baseline and after treatment for 72 h with healthy sera (n=6), SSc sera (n=6) or rh TGFβ1. Gel size in the different experimental conditions is expressed as percentage of baseline. Data are mean±SEM. *p<0.001 versus basal H-dMVECs.

Figure 5. Treatment with sera from patients with systemic sclerosis (SSc) induces changes in mRNA expression levels of endothelial and mesenchymal cell markers in healthy dermal microvascular endothelial cells (H-dMVECs). H-dMVECs were treated for 48 hours with sera from healthy subjects (n=6), sera from patients with SSc (n=6) or recombinant human transforming growth factor-β1 (TGFβ1; 10 ng/ml) and subsequently assayed for mRNA expression levels of *CD31*, *CDH5* (VE-cadherin), *FLI1*, *ACTA2* (α-SMA), *S100A4*, *SNAI1* (Snail1), *COL1A1* and *COL1A2* genes by quantitative real-time PCR. Ribosomal protein S18 (*RPS18*) mRNA was measured as an endogenous control for normalisation. The relative values compared with basal H-dMVECs are expressed as mean±SEM of three independent experiments performed with three H-dMVEC lines. *p<0.001 versus basal H-dMVECs.

Figure 6. Treatment with sera from patients with systemic sclerosis (SSc) induces changes in protein expression levels of endothelial and mesenchymal cell markers in healthy dermal microvascular endothelial cells (H-dMVECs). H-dMVECs were treated for 72 hours with sera from healthy subjects (n=6), sera from patients with SSc (n=6) or recombinant human transforming growth factor-β1 (TGFβ1; 10 ng/ml) and subsequently assayed for protein expression levels of CD31, VE-cadherin, Friend leukemia integration-1 (Fli1), α-smooth muscle actin (α-SMA), S100A4/fibroblast-specific protein-1 (FSP1), Snail1 and type I collagen. (A) Representative immunoblots are shown. Molecular weight values (kDa) are indicated. Protein expression of α-tubulin was measured as a loading control. Results are representative of three independent experiments performed with three H-dMVEC lines. (B-D) Representative fluorescence microphotographs show H-dMVECs double immunostained for the endothelial cell marker CD31 (red) and the myofibroblast marker α-SMA (green), or immunostained for Snail1 (red) and type I collagen (red). Nuclei are counterstained with 4',6-diamidino-2-phenylindole (DAPI; blue).

Treatment of H-dMVECs either with SSc sera or TGFβ1, but not with healthy sera, induces downregulation of CD31 in parallel with the appearance of α-SMA+ stress fibres, strong expression and nuclear localisation of Snail1 and de novo synthesis of type I collagen. Scale bar=20 μm. (E-G) The percentage of CD31/α-SMA double-positive cells (E), Snail1+ nuclei (F) and type I collagen+ cells (G) is reported in the histograms. Data are mean±SEM. *p<0.001 versus basal H-dMVECs.